KU LEUVEN

FACULTEIT GENEESKUNDE
BIOMEDISCHE WETENSCHAPPEN

Karakterisatie van motorneuronen afgeleid van geïnduceerde pluripotente stamcellen afkomstig van amyotrofe laterale sclerose patiënten met een FUS mutatie

Characterization of motor neurons derived from induced pluripotent stem cells of amyotrophic lateral sclerosis patients harbouring a FUS mutation

Masterproef voorgedragen tot het behalen van de graad van Master in de biomedische wetenschappen door

Joni VANNESTE

Promotor: Prof. dr. Ludo VAN DEN BOSCH
Co-Promotor: Prof. dr. Catherine VERFAILLIE
Begeleider: Wenting GUO

Leuven, 2015-2016

KU LEUVEN

FACULTEIT GENEESKUNDE
BIOMEDISCHE WETENSCHAPPEN

Karakterisatie van motorneuronen afgeleid van geïnduceerde pluripotente stamcellen afkomstig van amyotrofe laterale sclerose patiënten met een FUS mutatie

Characterization of motor neurons derived from induced pluripotent stem cells of amyotrophic lateral sclerosis patients harbouring a FUS mutation

Masterproef voorgedragen tot het behalen van de graad van Master in de biomedische wetenschappen door

Joni VANNESTE

Promotor: Prof. dr. Ludo VAN DEN BOSCH
Co-Promotor: Prof. dr. Catherine VERFAILLIE
Begeleider: Wenting GUO

Leuven, 2015-2016

Preface

I would like to thank my promoter prof. Dr. Ludo Van Den Bosch for giving me this opportunity and my supervisor Wenting Guo for her guidance. I am thankful to prof. Dr. Pieter Vanden Berghe and Dr. Werend Boesmans for helping me with the transport measurements. I am also grateful to Dr. Ann Swijsens for the electrophysiological data. I want to thank my co-promoter prof. Dr. Catherine Verfaillie and everyone of the Neurobiology lab. Special gratitude goes to Laura Fumagalli for the laughter's that we had together when the frustration was building up. I also want to express my lifelong gratitude to my father, who is my hero and died while fighting for one of the easiest thing that we do, breathing.

I used to take for granted the very air I breathe.
Now these days I am begging God for one last breath.
One last breath so that I may see my love ones face.
One last breath so I may smell spring flowers as they bloom.
One last breath so I may get a final taste of my favorite food.
One last breath so I may kiss my love goodbye.
I know with ALS I am asking for a lot when I ask for one last breath

Source: PoemHunter.com

Table of contents

List of abbreviations

ALS	Amyotrophic lateral sclerosis
BDNF	Brain derived neurotrophic factor
BMP	Bone morphogenetic protein
C9ORF72	Chromosome 9 open reading frame 72
Ca^{2+}	Calcium ions
Chat	Choline acetyltransferase
CI	Confidence interval
CNTF	Ciliary neurotrophic factor
C-terminal	Carboxy terminal
DAPI	4',6-diamidino-2-phenylindole
DMEM	Dulbecco's Modified Eagle Medium
DNA	Deoxyribonucleic acid
DRP(s)	Dipeptide repeat protein(s)
ER	Endoplasmic reticulum
ESCs	Embryonic stem cells
EWS	Ewing sarcoma
fALS	Familial ALS
FF	Fast-twitch fatigable
FR	Fast-twitch resistant
FTLD	Frontotemporal lobar degeneration
FUS	Fused in sarcoma
GDNF	Glial derived neurotrophic factor
Hb9	Homeobox transcription factor
HR	Homologous recombination
iPSCs	Induced pluripotent stem cells
Isl1	insulin gene enhancer protein1
LMN(s)	Lower motor neuron(s)
MN(s)	Motor neuron(s)
MND	Motor neuron disease
MNP	Motor neuron progenitor
mSOD1	Mutant SOD1
mRNA	Messenger ribonucleic acid
NEP	Neuroepithelial stem cell

NES	Nuclear export signal
NHEJ	Non-homologous end joining
NLS	Nuclear localisation signal
NMJ	Neuromuscular junction
N-terminal	Amino terminal
PBS	Phosphate buffered saline
RA	Retinoic acid
RAN	Repeat associated non-ATG
RNA	Ribonucleic acid
RNP	Ribonuclear protein
ROS	Reactive oxygen species
SAG	Smoothened agonist
sALS	Sporadic ALS
Shh	Sonic hedgehog
sMN(s)	Spinal motor neuron(s)
SMA	Spinal muscular atrophy
SMN	Survival of motor neuron
snRNP	Small nuclear ribonuclear proteins
SOD1	Superoxide dismutase 1
SR	Slow-twitch fatigue resistant
TAF15	TATA-binding protein-associated factor 15
TARDBP (gene)/ TDP-43 (protein)	Tar DNA binding protein
UMN(s)	Upper motor neuron(s)
UPR	Unfolded protein response
WT	Wild-type
ZnF	Zinc finger motif
B-ME	Beta-mercapto-ethanol
βIII-tub.	Beta III-tubulin

Dutch summary:

ALS	Amyotrofe laterale sclerose
fALS	Familial ALS
iPS cellen	Geïnduceerde pluripotente stamcellen
MN(n)	Motorische neuron(en)
NES	Nucleair export signaal
NLS	Nucleair lokalisatie signaal
sALS	Sporadische ALS
sMN(n)	Spinal motor neuron(en)

Abstract

Amyotrophic lateral sclerosis (ALS) is a devastating adult-onset neurodegenerative disease characterized by the progressive loss of motor neurons in the brain and spinal cord. A greater understanding of early disease mechanisms is needed to create new therapeutic targets. Although plenty of animal models were generated, most of these models don't fully mimic the pathological changes seen in ALS patients. In this thesis, induced pluripotent stem cells (iPSCs) obtained from ALS patients harbouring a mutation in the nuclear localization signal (NLS) of fused in sarcoma (FUS) (P525L, R521H) and two healthy controls were used to investigate FUS-associated ALS. Both healthy control and ALS-patient specific iPSC lines were successfully differentiated into spinal motor neurons and consistent with clinical observations, typical FUS cytoplasmic mislocalization was detected in FUS-P525L and FUS-R521H cell lines. Moreover, based on MitoTracker staining and time-lapse imaging a disturbance in mitochondrial transport was observed in patient iPSC-derived mature MNs. In addition, performing time-lapse imaging in combination with a LysoTracker staining, suggested lysosomal deficits in ALS patient-derived MNs. These data implicate transport defects as a pathological mechanism in mutant FUS associated ALS. This thesis also demonstrated the potential of using human MNs derived from iPSCs as a model for studying ALS.

Chapter 1: Introductory overview of the literature

1.1 Amyotrophic Lateral Sclerosis

1.1.1 ALS is a disease of upper and lower motor neurons

Amyotrophic lateral sclerosis (ALS), also known as Lou Gehrig's disease, is a fatal adult-onset neurodegenerative disorder in which **motor neurons (MNs) progressively degenerate**. Both upper motor neurons (UMNs) in the motor cortex and lower motor neurons (LMNs) in the brainstem and spinal cord are involved (1). Due to this loss of MNs the patients suffer from spasticity, muscle weakness and muscle atrophy. As this MN degeneration gradually spreads, the patients become progressively paralyzed, and the entire body becomes involved (2). Death of the patient is usually due to respiratory failure and this within an average of 2 to 5 years after first symptom onset (3). However, the variability in disease duration is large, with some patients dying within months after onset and others surviving for more than twenty years (1). The oculomotor, sensory and autonomic functions of ALS patients are not affected (4).

The name describes the key features of the disease. "Amyotrophic" refers to the muscle atrophy, which results in the LMNs signs: muscle weakness and fasciculations (3). "Lateral sclerosis" refers to hardening of the spinal cord lateral columns as axons from MNs in these areas degenerate and are replaced by **gliosis**. The clinical results are UMN signs: spasticity, overactive reflexes, dysphagia and dysarthria (3). Besides the selective MN degeneration, the presence of **ubiquitinated inclusions** in the remaining degenerating MNs and glia cells is another main neuropathological hallmark of ALS (5). Cytoplasmic inclusions containing ubiquitinated and phosphorylated TAR DNA binding protein 43 (TDP-43) is the most common histopathological hallmark of ALS (5).

ALS is traditionally classified into two categories: **familial ALS** (fALS) and **sporadic ALS** (sALS). Although ALS is predominantly a sporadic disease (sALS), approximately 10% of ALS cases have a family history of ALS, indicating genetic inheritance (fALS) (6). In most cases of familial ALS there is an autosomal dominant pattern of inheritance. Mutations in more than twenty genes, including *SOD1*, *FUS*, *TARDBP* and *C9ORF72* (see genetics) are known (7). Although in a small number of sALS cases mutation-associated causes have also been identified, the etiology of sALS remains elusive in the majority of cases (Fig. 1). Sporadic ALS is thought to arise from a combination of aging, genetic susceptibility and environmental factors, although no definitive environmental risk factors have been identified yet (8). FALS and sALS are clinically indistinguishable, suggesting that it is the same disease (7).

With an incidence of approximately 1-5 cases per 100,000 per year, ALS is the **most common form of motor neuron disease** (MND) in adults (2). There is a slightly higher incidence in men than women (M:F ratio: 1,54) with a life time risk of 1/472 for women and 1/350 for man at the age of 70 (9). As a result of the rapid disease progression, the prevalence of ALS is relatively low, namely at around 5.2 per 100,000 (10). This neurodegenerative disorder is an adult-onset disease with 55 years as the mean age of onset (11). Juvenile ALS (<25 years) is rare (1).

Treatment remains essentially supportive, since **no effective therapy** is available. The fact that the only drug on the market, riluzole, prolongs survival of ALS patients by only a few months (12), emphasizes the need for new therapeutic strategies. Animal models of ALS have been instrumental to our current knowledge of ALS. However, therapeutics developed using these animal models do not readily translate into the clinic. The use of patient-derived induced pluripotent stem cells (iPSCs) could complement existing models and facilitate clinical translation (13).

1.1.2 Genetics

An important breakthrough in ALS research was the discovery of the first ALS gene, *SOD1*, in 1993 (14). In the last twenty years a number of new ALS-causing genes were identified (for an overview see: (4)). These genetic discoveries play an important role in our understanding of the pathological pathways in ALS. I will focus on four causative genes: *SOD1*, *TARDBP*, *FUS* and *C9ORF72* that account together for more than half of the fALS cases (Fig.1).

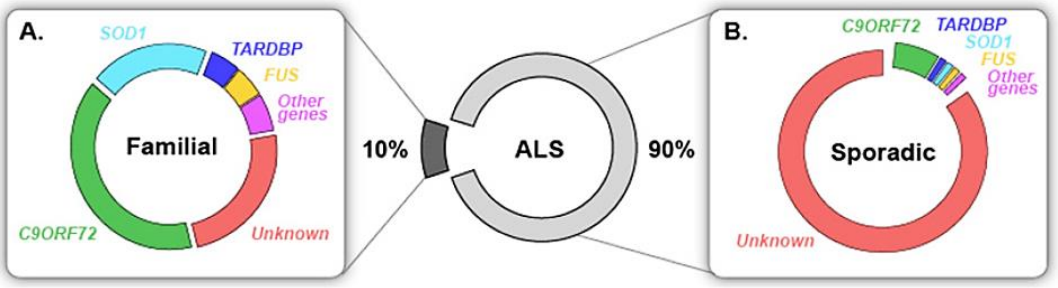

Figure 1. Known genetic causes in familial and sporadic ALS. **A.** 20% of fALS are caused by mutations in SOD1. Mutations in the DNA/RNA-binding proteins TDP-43 and FUS cause each ~4% of fALS. Hexanucleatide repeat expansions in *C9ORF72* are the most common genetic cause of ALS accounting for almost 40% of fALS in people of European ancestry. Several other genes have been identified as genetic causes of ALS and collectively today over 60% of fALS can be explained by known mutations. **B.** While the aetiology in the majority of sALS remains unknown, mutations in genes known to cause fALS were identified in a small fraction of apparently sporadic patients. Figure is adapted from the review of Laferrière F. and Polymenidou M. (2015) (5).

Superoxide dismutase 1 (SOD1)

Mutations in the *SOD1* (superoxide dismutase 1) gene were the first identified genetic cause of ALS (14). SOD1 protects the cell against reactive oxygen species (ROS) by converting superoxide radicals

into hydrogen peroxide (15). More than 160 mutations, spread throughout the gene, have been reported. Almost all are dominant missense mutations and together these mutations account for 20% of fALS and 2-3% of sALS cases (15). The identification of the *SOD1* gene as a genetic cause of ALS led to the engineering of transgenic rodent models overexpressing the human mutant SOD1 (mSOD1) protein. These mSOD1 animal models, with $SOD1^{G93A}$ mice as most important one, formed the basis of much of our understanding of ALS pathogenesis (10). The role of non-neuronal cells in ALS pathology is one of these important findings (10). However, 20 years after the discovery of the *SOD1* mutations no consensus has emerged about how mutant SOD1 leads to ALS. Even more, the pathology of mutant SOD1-ALS is now suggested to be distinct from that of all other types of ALS, as it lacks the TDP-43 and/or FUS pathology present in all the other ALS types (16).

TAR DNA-binding protein (TDP-43)

The *TAR-DNA binding protein* (*TARDBP*) gene encodes the protein TDP-43, which is the major component of the cytoplasmic ubiquitinated inclusions bodies found in the majority of ALS patients (5). TDP-43 is not only a pathological hallmark of ALS but also a genetic cause. Mutations in *TARDBP* cause an autosomal dominant form of fALS and account for ~4% of fALS and ~1% of sALS cases (6). More than 40 missense mutations have been associated with ALS, and the majority resides in the C-terminal region. These mutations causes the accumulation of TDP-43 in the cytoplasm and its exclusion from the nucleus, providing an almost exact parallel with FUS mutations (see below) (17). This altered intracellular localization of TDP-43 and FUS is thought to contribute to their toxicity (17). TDP-43 is an DNA/RNA binding protein and plays a crucial role in transcription, alternative splicing, mRNA stability and microRNA processing (18). The central role of TDP-43 in ALS pathogenesis has highlighted the importance of RNA processing. Additional support for this hypothesis comes from the discovery of mutations in FUS and hexanucleotide repeats in C9ORF72 (see below).

Fused In Sarcoma/translated in liposarcoma (FUS/TLS)

Shortly after the discovery of the TDP-43 mutations, mutations in the *fused in sarcoma/translated in liposarcoma gene* (*FUS/TLS* or just *FUS*), encoding the protein FUS, were discovered (17). Mutations in this gene account for ~4% of fALS cases and ~1% of sALS cases (6). The discovery of FUS mutations caused considerable excitement in the field of ALS because the protein shares functional and structural similarities with TDP-43 (19). FUS is also a DNA/RNA binding protein with multiple cellular functions including transcription, maintenance of genomic stability and mRNA processing and transport (Fig. 2) (20). It is presently not clear whether TDP-43 and FUS act through common or divergent pathways. A common genetic pathway for FUS and TDP-43 has been suggested, with FUS

possibly acting downstream of TDP-43 (21). However, it is remarkable that TDP-43 and FUS neuronal inclusion do not overlap (22). In FUS-associated cases the ubiquitinated protein inclusions have been demonstrated to be immunopositive for the FUS protein but not for TDP-43 (5). In contrast, TDP-43 pathology has been observed in almost all ALS patients, except of patients with fALS-FUS and fALS-SOD1 (5). Another hypothesis is that a small set of common targets of FUS and TDP-43 may contribute to ALS pathogenesis (23). For example, both TDP-43 and FUS interact directly and indirectly respectively with Drosha, a protein involved in primary miRNA processing (24). Additionally, in both proteins prion-like domains have been identified and this has been implicated in TDP-43 and FUS toxic misfolding and aggregation (25). It is not yet clear whether a loss of normal FUS function in the nucleus, a gain of toxic properties in the cytoplasm or a combined effect plays a role in FUS pathology (26).

Chromosome 9 open reading frame 72 (C9ORF72)

An hexanucleotide (GGGGCC) expansion in the non-coding first intron of *C9ORF72* has been identified to be responsible for approximately 40% of fALS and 7% of sALS cases (27). This gene encodes a protein with an unknown function. However, a crucial role in neuronal activities such as axonal transport and the autophagy-lysosome process has been suggested (28). Not only accounts this gene for a high percentage of fALS (~40%) and sALS (~7%), this is also the first time that a large intronic repeat expansions was implicated in ALS. This supports the hypothesis, based on TDP-43 and FUS, that RNA metabolism disruption plays a crucial role in ALS pathogenesis. The $(GGGGCC)_n$-rich RNA transcripts are able to form highly stable RNA G-quadruplexes (29). These G-quadruplex-folded C9ORF72 transcripts accumulate within nuclear foci where they might lead to sequestration of RNA-binding proteins away from their normal RNA targets and as a consequence might lead to the disrupting of normal RNA processing (30). Two other hypotheses to explain how C9ORF72 mutations could cause disease were proposed. Loss of function of the *C9ORF72* gene product (haploinsufficiency) and the generation of toxic dipeptide repeat proteins (DRPs) by repeat associated non-ATG (RAN) translation of the sense and antisense transcripts (31).

1.1.3 ALS is a complex and multifactorial neurodegenerative disease

Untill today, the exact mechanism underlying the selective MN degeneration in ALS is far from being understood. The current hypothesis is that ALS is the result of a complex interplay between multiple pathogenic cellular mechanisms (32), including excitotoxicity, oxidative stress, mitochondrial dysfunction, impairment of axonal transport, protein aggregation, endoplasmic reticulum (ER) stress,

neuroinflammation and abnormal RNA processing (10). Although each of these factors is individually well known, their temporal interplay and contribution to the disease remains elusive.

Glutamate-induced excitotoxicity has been linked to the pathogenesis of ALS since the discovery that the cerebrospinal fluid of a subset of ALS patients showed increased extracellular glutamate level (33). Excitotoxicity is a pathological process in which neuronal death is caused by overstimulation of the post-synaptic glutamate receptors (AMPA and NMDA-receptors), which leads to a toxic rise in intracellular calcium (Ca^{2+}), followed by aberrant activation of proteases, lipases, phospholipases and endonucleases and eventually in cell death (34–36). The only FDA-approved therapy for ALS, riluzole, has anti-excitotoxic properties (37). However, the fact that riluzole prolongs the survival of ALS patients by only a few months (12), suggests that there are additional pathological mechanisms involved. Besides an increased glutamate level, increased **oxidative stress** is observed in sALS patients (38). This indicates that oxidative damage, due to increased levels of free radicals, could be an additional pathologic factor. Mitochondria are the main source of ROS and **disturbances of the mitochondrial functioning** is thought to be an important factor in the pathogenesis of ALS. Mitochondria are essential for the survival and functioning of neurons since they are necessary for energy and Ca^{2+} buffering (39). In addition, mitochondria play a central role in controlling apoptosis (40). Thus, mitochondrial dysfunction can lead to bioenergetics failure, oxidative stress and apoptosis (41). A reduced mitochondrial DNA content associated with increased mutations of mitochondrial DNA and a disturbance of the respiratory chain has been demonstrated in ALS-patients (41). Moreover, in both ALS patients and animal models an abnormal morphology and an altered distribution of mitochondria have been observed (42–44). **Axonal transport** is essential for mitochondrial quality control by supplying functional mitochondria to the axon and by removing damaged or aged mitochondria out of the axon. In this way damaged mitochondria are able to undergo mitophagy (autophagy of mitochondria) in the soma, before they release harmful ROS (45). Mitophagy also occurs at the distal part of the axon and therefore retrograde transport of the formed autophagosomes is essential (45). The necessity of axonal transport of mitochondria and other organelles or proteins becomes particularly important in the context of the huge axons of MNs, which can extend a great distance from the cell body (more than 1 m in humans) (46). Therefore, failure of mitochondrial quality control due to axonal transport defects would occur first at the distal end of the axon (see dying-back hypothesis). Additionally, deregulated axonal transport of lysosomes can give rise to accumulation of **protein aggregates**. Protein aggregation is a common hallmark of all types of ALS (32) and the trigger for this protein aggregation is thought to be protein misfolding caused by mutations, protein damage or protein seeding (1). However, it remains unclear whether inclusion formation is responsible for cellular toxicity, whether protein aggregates are the

consequence of neurodegeneration or whether it is a protective reaction of the cell to reduce intracellular concentrations of toxic proteins (10). Protein aggregation could be toxic for MNs because they can physically block the transport of other proteins, organelles and vesicles (47). Moreover, the formation of protein inclusions disrupts the function of entrapped proteins, such as proteins that are critical for the viability of the neuron (32,48). The identification of two DNA/RNA-binding proteins, TDP-43 and fused in sarcoma (FUS), as components of cytoplasmic protein inclusions in ALS patients focused the attention to **RNA processing alterations** as an important pathophysiological mechanism in ALS (1). Increased cytoplasmic aggregation of FUS and TDP-43 results in nuclear depletion of these proteins, which can induce abnormalities of RNA processing (49,50). Accumulation of misfolded proteins elicits the **ER stress** response, followed by activation of the unfolded protein response (UPR) and ultimately in the activation of apoptotic pathways when the UPR is exhausted (51). Several evidence implicates ER stress as an important feature of MN degeneration in ALS, such as the finding that UPR markers are upregulated in sALS patients (52) and in mSOD1 rodent models (53). It is also generally accepted that ALS pathogenesis is not confined to neurons, but that neighboring glial cells also play a crucial toxic role in the observed MN degeneration (10). For example, at the sites of MN injury, **neuroinflammation** is a prominent pathological finding and is characterized by the activation of microglia, which could further contribute to neurodegeneration (54).

1.1.4 Axonal transport defects and the dying-back hypothesis for ALS

Intriguingly, altered function of the most distant cellular sites (axons and synapses) often occurs during initial stages of disease, before any MN loss and before disease onset (55). The **"dying-back" hypothesis** for ALS is based on this observation and states that: "motor neuron pathology begins at the distal axon and proceeds in a "dying back" pattern" (55). Additionally, the longest and largest nerve fibers with the highest metabolic demand seem to be the most susceptible to the "dying back" phenomenon (55). This suggests that the "dying-back" pattern might be due to size-depended undernourishment of the distal axon (56,57), which can provide an explanation for the selective MN vulnerability seen in ALS. Moreover, this concept of "dying-back" suggests a **key role for axonal transport** defects in the pathological mechanisms of ALS.

Although axons can represent 99% of the cell volume, it is the cell body of MNs that is the primary site of metabolic functions and degradation (58). This polarity of MNs makes them particularly dependent on active axonal transport (46). Newly synthesized proteins, lipids and organelles, such as mitochondria and lysosomes, must continuously be supplied to the axon (anterograde transport). Whereas, transport from the cell periphery to the cell body (retrograde transport) clears misfolded or

recycled proteins and damaged organelles from the axon (59). Apart from its role in neuronal metabolism, axonal transport is essential for long-distance signalling of trophic and stress signals from the distal axon to the soma (59). The main mechanism of axonal transport is along microtubules through the action of molecular motors (60). Molecular motor proteins are enzymes that use the energy of ATP hydrolysis to move cargos along the cellular cytoskeleton (47). Kinesin and dynein are the molecular motors responsible for fast axonal transport and are mainly responsible for anterograde and retrograde transport, respectively (60). Evidence of axonal transport defects in ALS patients emerged from electron microscopy studies that revealed the presence of swellings in the initial segment of motor axons of patients with ALS. These swellings contain various cargos of motor proteins, such as vesicles, lysosomes, mitochondria and intermediate filaments (42). Additionally, a significant defect in both anterograde and retrograde transport is observed in the mutant $SOD1^{G93A}$ transgenic mouse model (61,62). Time-course studies indicate that the inhibition of retrograde transport is one of the earliest pathogenic events apparent in the mutant $SOD1^{G93A}$ ALS model (63), suggesting that slowing of axonal transport is an early event in the pathogenesis of ALS. The idea that defective axonal transport can directly trigger neurodegeneration is strongly supported by the identification of mutations in motor proteins in patients with neuropathies (47,59). Experimental findings in a mouse model in which microtubule assembly is affected, the *pmn* model, provides additional evidence that primary axonal pathology may lead to a MND phenotype and for the involvement of axonal transport defects (55,64). Rescuing only MN cell bodies and not axonal degeneration, by overexpression of anti-apoptotic Bcl2, did not prolong survival (65). In contrast, preventing axonal degeneration resulted in a prolonged survival (66). That defects in axonal transport are sufficient to cause MN neurodegeneration is also supported by the observation that disruption of the function of the cytoplasmic dynein/dynactin complex causes MND with MN degeneration and muscle atrophy similar to ALS (59,67). In addition, two different mouse strains, Legs at odd angels (*Loa*) and cramping (*Cra1*), that are each heterozygous for a mutation in the cytoplasmic dynein heavy chain 1 (DynC1H1), exhibit an age related progressive loss of muscle function and motor coordination (68). Other evidence for a role of defective axonal transport in MNDs is the development of a late-onset progressive MND in transgenic mice expressing dynamitin (69). The overexpression of dynamitin disassembles dynactin and disturbs dynein function, resulting in an inhibition of retrograde transport (69).

1.2 The role of FUS in ALS

FUS was first identified because of its oncogenic properties following a chromosomal translocation resulting in the fusion of the N-terminus of FUS, which is shown to function as a transcriptional

activation domain, with the transcription factor CHOP (70). The FUS gene is located at 16p11.2 and contains 15 exons encoding a 526 amino-acid protein (71). FUS belongs to the FET protein family, which also includes two other structurally and functionally similar proteins, EWS (Ewing sarcoma) and TAF15 (TATA-binding protein-associated factor 15). This family represents a class of proteins that functions at all stages of gene expression, from transcription to protein translation (72).

1.2.1 Structure

The amino terminus (N-terminal) of the FUS protein contains a Gln-Gly-Ser-Tyr (QGSY)-rich domain with transcriptional activation activity and prion-like properties (Fig. 2). In addition, the FUS protein contains multiple domains that can bind to nucleic acids: a Glycine-rich domain, a RNA-recognition motif (RRM), which contains a nuclear export sequence (NES), and two Arg-Gly-rich repeat regions which flank a zinc-finger region (ZNF). This is followed by a highly conserved non-classical **nuclear localization signal** (NLS) (Fig. 2) (73). The NLS is recognized by transportin 1, which is required for the import of FUS into the nucleus (49). Under physiological conditions wild type (WT) FUS is predominantly localized in the nucleus, although FUS can engage in nucleo-cytoplasmic shuttling under influence of the NES and NLS (74). Over 50 different *FUS* mutations have been identified in ALS patients. Most of these mutations are missense mutations with an autosomal dominant inheritance pattern (26). Two-thirds of the FUS mutations are located in exons 12-15, with the majority in the NLS itself (Fig. 2) (26). These C-terminal mutations have proven to be pathogenic by disturbing or entirely deleting the NLS, which causes an aberrant cytoplasmic localisation of FUS (49). The remaining one-third are located in exons 3-6, which encode the SYGQ-rich and Gly-rich regions (Fig. 2) (26). Mutations in this region are mainly associated with sALS, in contrast to C-terminal mutations that have a higher frequency in fALS cases (26).

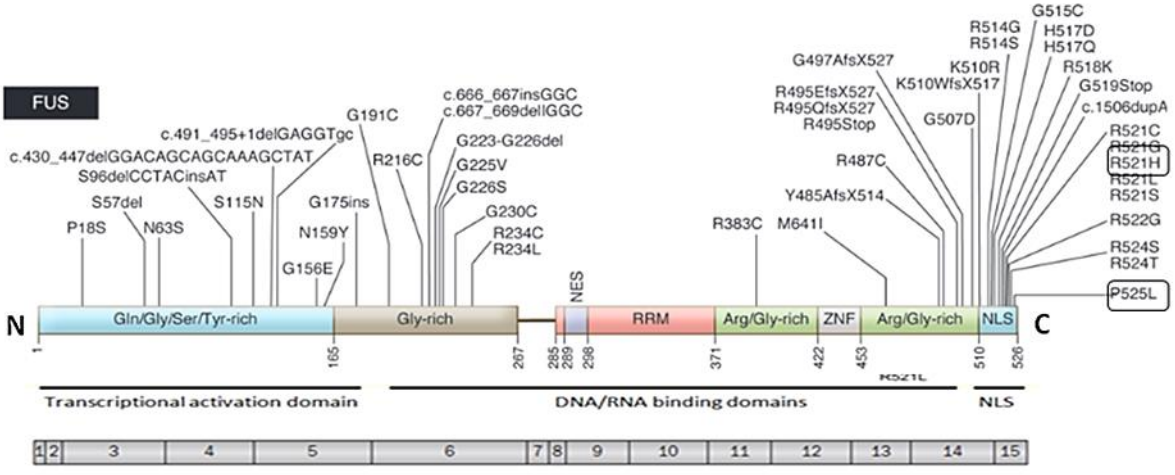

Figure 2. Domain organisation of the FUS protein and ALS-associated mutations. FUS is composed of an N-terminal region rich in Gln-Gly-Ser-Tyr (QGSY) that possess transcriptional and prion-like activity (light blue), a Gly-rich region rich (brown), a RNA recognition motif (RRM, red) containing a nuclear export signal (NES), two regions rich in Arg-Gly (green) flanking a zinc finger motif (ZNF, white) and a C-terminal nuclear localisation signal (NLS, blue). Numbers under the protein-line indicate the boundaries of each domain. The corresponding exons are indicated in the lower part of the figure. Identified ALS causing mutations in FUS are shown. Most mutations are clustered in the C-terminal region of FUS, disturbing the NLS. IPSCs derived from ALS patients with the mutations R521H and P525L (black squares) are used in this thesis. This figure is adapted from the review of Peters *et al.* (2015) (73).

1.2.2 Physiological functions of FUS in neurons

FUS is a **DNA/RNA-binding protein** that has been implicated in a wide range of cellular processes, including DNA repair, transcriptional regulation, mRNA processing and RNA transport (Fig. 3). The FUS protein directly binds single- and double-stranded DNA and several functions in the context of DNA processing are suggested (75). First, FUS binds to the promoter of more than one 1000 genes and associates with RNA polymerase II, regulating its transcriptional activity (19,75). This suggests that FUS influences **transcription initiation** (Fig. 3). This is also supported by the observation that the fusion protein consisting of the N-terminal part of FUS and the C-terminal part of the DNA-binding transcription factor CHOP, has strong transcriptional activity and plays a role in cancer (70). Second, FUS plays a direct role in the **DNA repair** of double-stranded DNA breaks, including homologous recombination (HR) and non-homologous end joining (NHEJ) (Fig. 3) (75). It is suggested that the C-terminal region of FUS is implicated in the DNA-repair capacity of FUS. Moreover, a majority of ALS-causing mutations are located within the C-terminus of FUS which raises the possibility that these mutations interfere with the DNA-repairing function of FUS (75). This notion is supported by the observation that FUS knockout (FUS-/-) mouse models reveal signs of genomic instability (76). Third, the FUS protein binds telomeric DNA and may be important for T-loop formation and the modulation of the telomeric length (75). Dysfunctional telomeres have been pathologically linked to Alzheimer's and Parkinson's disease and may also be relevant to other neurodegenerative diseases (77).

Beyond DNA transcription and repair, FUS is involved in a wide range of RNA-related cellular processes, including **pre-mRNA spicing and mRNA export** (Fig. 3) (20). It has been shown that the nucleo-cytoplasmic shuttling of FUS is functionally linked to transport of mRNA from the nucleus to cytoplasm (74). In addition, FUS is part of the spliceosome machinery and directly binds to splicing components (78) and to many transcripts in the brain (79) (Fig. 3). FUS also plays a role in micro-RNA processing by indirectly interacting with Drosha (Fig. 3) (80). Additionally, FUS binds to long non-coding RNAs (Fig. 3) (31).

Besides clear nuclear functions like transcription and mRNA splicing, FUS has cytoplasmic functions as well (Fig. 3). These include **mRNA transport** to dendritic spines for local translation, suggesting a role of FUS in neuronal plasticity (81). Besides playing a role in mRNA transport, FUS proteins are also incorporated into **stress granules**, in which they control mRNA stability and translational efficiency (82).

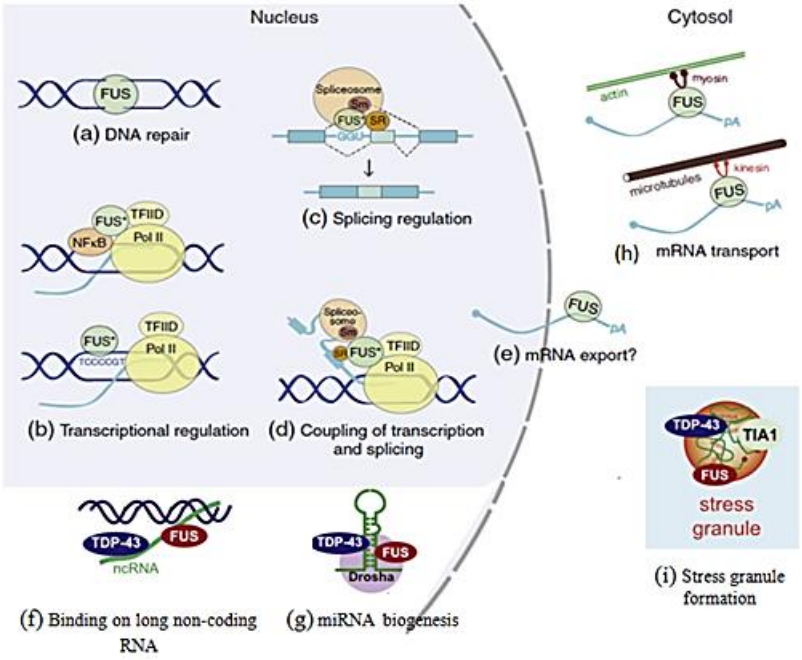

Figure 3. Physiological functions of FUS in neurons. Proposed roles of FUS in DNA/RNA metabolism in the nucleus and cytoplasm. **(a)** FUS has DNA homologous pairing activity and is important for the repair of DNA double strand breaks. **(b)** FUS interacts with RNA polymerase II and directly binds to specific DNA sequences in the promoter region of certain target genes (TCCCCGT), suggesting a role of FUS in regulating gene expression. **(c)** FUS affects alternative splicing by interacting with intronic regions near splice sites and subsequently recruiting the spliceosome or other splicing factors. **(d)** FUS interacts with both the transcriptional machinery and the splicing machinery and therefore has been proposed to couple transcription to translation. **(e)** FUS plays a role in mRNA export by shuttling between the nucleus and cytoplasm. **(f)** FUS binds to long non-coding RNAs. **(g)** FUS plays a role in miRNA processing by binding to Drosha. **(h)** FUS is involved in transport of specific mRNAs for local translation into dendrites and dendritic spines. **(i)** FUS is incorporated into stress granules, in which they form complexes with other RNA-binding proteins and mRNAs. This figure is adapted from the review of Dormann *et al*. (2013) (83) and *Ling et al*. (2013) (31).

1.2.3 Pathology

Although, mutations in the FUS gene only account for a small fraction of fALS cases (see genetics), the FUS protein seems to have a general role in the pathogenic mechanism of neurodegenerative disorders. **Mutations in the FUS gene** have been identified as causative or risk factors for several other neurodegenerative diseases besides ALS, including essential tremor and frontotemporal lobar degeneration (FTLD) (26). Moreover, *de novo* FUS mutations seem to be the most important genetic cause of early-onset ALS (84). In addition, **FUS aggregates** have not only been observed in neurons of

patients with ALS, but also in FTLD-FUS and polyglutamine diseases, such as Huntington's disease (26). These inclusions are typically observed in the cytoplasm and (less frequently) in the nucleus (26). However, the morphology and distribution of FUS inclusions differs across different diseases entitie s(85).

The underlying pathogenic mechanism(s) leading to FUS-mediated neurodegeneration is largely unknown. However, it has been observed that ALS-linked mutant forms of the FUS protein cause defects in nuclear import, which lead to **cytoplasmic mislocalization of FUS** (49). This imbalance may interfere with the physiological functions of FUS in the nucleus (loss of function) or/and cause a toxic gain-of-function of the FUS protein aggregates in the cytoplasm. Moreover, it was observed that the degree of cytoplasmic displacement of the protein is correlated with the severity of the clinical presentation and age of onset (49,86,87). However, the way in which impaired nuclear import of FUS mediates neurodegeneration remains to be elucidated. It has been suggested that mislocalization of FUS to the cytoplasm is presumably the first hit in the pathophysiological cascade that leads to neurodegeneration (83). A second hit, such as cellular stress and/or defects in protein degradation, is suggested to be necessary (83). The formation of stress granules, with cellular stress as the second hit, and transformation into insoluble protein deposits is one of the possibilities (83). Under conditions of stress or in response to toxic insults, endogenous FUS is redistributed to the cytoplasm and is assembled into stress granules (88), which are ribonucleoprotein (RNP) assemblies that induce translational arrest of most cellular mRNAs to ensure specific production of stress-involved proteins (89). Stress granules are very dynamic and reversibly assemble and disassemble in normal conditions. It is hypothesised that the inability to disassemble these structures is a pathological mechanism involved in ALS (90). Both types of FUS mutations (in the N-terminal part and in the C-terminal part) are thought to contribute to this phenomenon either directly by increasing the aggregation propensity (mutations N-terminal region) (91) or indirectly by increasing the concentration of FUS in the cytoplasm (mutations disturbing the NLS) (49). The observation that stress granule markers are present in inclusions from patients with ALS-FUS or FTLD-FUS supports the hypothesis that FUS-positive stress granules could be the precursors to these protein aggregates (49). In addition to cytoplasmic inclusions, cytoplasmic mislocalization can lead to a loss of the nuclear functions of FUS, such as transcription and alternative splicing. In view of the high frequency of alternative splicing in the brain, a role of an altered alternative splicing pattern has been suggested in FUS-mediated pathology (79). Gene ontology analysis of all putative transcript targets of FUS suggested a role of disturbances of axonal growth and the cytoskeletal network in the pathological mechanism of FUS (79). An altered splicing of axonal and cytoskeletal-related transcripts causes deteriorated axonal maintenance and repair, which could make the MNs more sensitive for aging and stress (79). The

observations that FUS facilitates miRNA processing through indirect Drosha interactions in the nucleus (80), and the necessity of a functional miRNA pathway for maintaining normal neuronal lifespan (92) and homeostatic functions in glia-cells (93), introduces another hypothesis: the disturbance of a functional miRNA pathway by decreasing the amount of FUS protein in the nucleus (24).

Besides this, many ALS-causing mutations have also been reported to be localized in the QGSY and Gly-rich region of FUS (Fig. 2). It is suggested that these mutations do not perturb the NLS (94). However, these mutations can cause loss of transcriptional activity of FUS by disturbing FUS assembly and chromatin binding (95). Additionally, given the high aggregation tendency that is predicted for the QGSY region (25), the formation of **intranuclear aggregates** of FUS is proposed as an alternative hypothesis (94). The formation of these aggregates can result in loss of physiological functions of FUS and possible cytotoxic effects. In addition Nomura *et al*. observed that the amyloid-like fibrillary aggregates that are formed by these mutant FUS proteins function as efficient seeds to trigger the aggregation of WT FUS proteins. This finding supports the **prion hypothesis**: misfolded FUS propagates from cell to cell in a prion-like manner, which may represents the mechanism for the relentless disease progression (25).

1.3 Induced pluripotent stem cell-derived neurons as a new disease model for ALS

The inability to obtain sufficient quantities of affected patient tissues is a big obstacle towards the understanding of the pathogenic pathways of neurological diseases. To overcome this challenge **animal models of ALS** have been generated to perform mechanistic studies or drug screenings (96). Numerous transgenic models have been based on (over)expressing of genetic mutations described in fALS cases (13), including yeast, *Drosophila*, nematode, zebrafish, mouse and rat models of SOD1, TDP-43, FUS and C9ORF72. The most popular animal model for ALS is the transgenic mouse model expressing the mutant form of the human *SOD1* gene (G93A)(97). Despite the observation that these models show similar pathological events as in patients and despite the fact that these *in vivo* models learned us a lot about the pathological mechanisms of ALS, there has been a striking **failure to translate experimental observations into successful clinical results** (10,96–98). This might be due to genetic and anatomical variations between human and animals. In particular, mutant SOD1 transgenic mice often require a several-fold overexpression of mutant SOD1 proteins to produce a phenotype, as opposed to a single copy in fALS patients (96). This overexpression of mSOD1 proteins can produce artifacts not relevant to human ALS pathogenesis (96). Also, more than 90% of the ALS patients have a sporadic form of the disease thought to arise from complex interactions between

environmental factors and numerous low risk susceptibility loci (99). This limits the potential of animal models in recapitulating the most common form of ALS. The many negative results observed in clinical trials raise the question about the suitability of current ALS-models. As a consequence, iPSCs could offer a new way to analyze the pathological mechanisms involved in ALS.

Human induced pluripotent stem cells provide the opportunity to study mechanisms of neurodegeneration in a model with naturally occurring pathology in a human genetic background. Yamanaka and colleagues were the first to show that human iPSCs can be generated by transducing adult human dermal fibroblast with viral vectors carrying the pluripotent transcription factors *Oct4*, *Sox2*, *Klf4* and *c-Myc* (100). The iPSCs generated in this manner share the main properties of embryonic stem cells (ESCs), which include unlimited self-renewal while preserving their potential to differentiate into the three embryonic germ layers (100,101). Owing to their ESC-like pluripotency, iPSC lines derived from ALS patients allow the production of numerous cell subtypes such as neurons, astrocytes, oligodendrocytes and Schwann cells (13) that contain the genetic information of individual patients (102). This gives us the opportunity to investigate the involvement of different cell types in disease pathogenesis and the selective susceptibility of MNs in ALS.

Differentiation of iPSCs into MNs *in vitro* is based on replicating MN development *in vivo* (101,103). In this thesis, we focused our attention exclusively on spinal MNs (referred to hereafter simply as MNs). Figure 4 shows the fundamental steps regulating MN development *in vivo* (101). During gastrulation, inhibition of bone morphogenetic protein (BMP) signaling by factors derived from the Spemann-Mangold organizer (noggin, chordin, follistatin) is required to induce neuronal fate in the dorsal region of the ectoderm (104) (Fig. 4A). Additional inductive signals, including Wnt-signaling have also been identified to play a role in the specification of neuroectoderm (105) (Fig. 4A). Following neuronal induction, the neuronal tube is specified along both the rostral-caudal (Fig. 4A) and the dorso-ventral axes (Fig. 4B) by signaling gradients that act as positional cues (101,103). Along the rostral-caudal axis, the neuronal tube is specified into the major components of the CNS, including brain, midbrain, hindbrain and spinal cord (101). The major signal that contribute to the caudalization of the neurons to induce spinal cord identity is retinoic acid (RA) (101). Once the spinal cord is specified, continued release of RA from the somites in combination with a gradient of sonic hedgehog (Shh) secreted from the notochord and cells of the floor plate and BMP signaling from the roof plate provides patterning along the dorso-ventral axis. RA and Shh signalling act together to induce ventralization (MN identity) of the spinal cord stem cells (101). *In vitro*, the induction of above mentioned developmental signals are used to guide iPSCs into MNs (101,103).

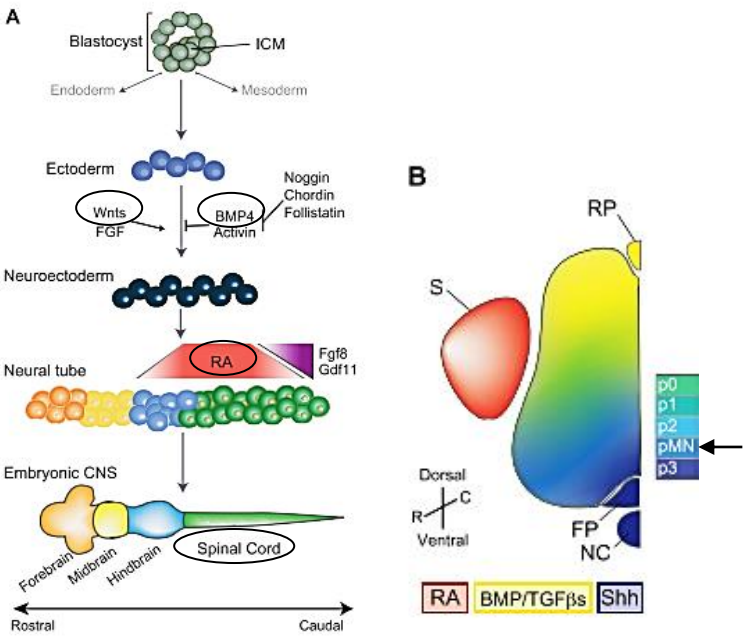

Figure 4. **Spinal cord development (A) and motor neuron specification (B) *in vivo*. (A)** In the dorsal region of the ectoderm neuroectoderm is specified through the inhibition of BMP and activin signalling and enhanced FGF and Wnt signalling. The neuronal plate is then patterned along the rostro-caudal axis by a gradient of retinoic acid (RA). RA signalling induces caudalization (spinal cord identity). **(B)** The spinal cord is also patterned along the dorso-ventral axis through a combined action of RA, Sonic hedgehog (Shh) and BMP signalling. Ventralization (MN identity) is established by RA and Shh signalling. Somites (S), floor plate (FP), nototchord (NC), roof plate (RP). Figure is adapted from the review of Davis-Dussenbery *et al*.(2014) (101).

The question remains how good iPSC-derived cells recapitulate *in vivo* biology and, ultimately, the fidelity of the neurodegenerative disease process seen in ALS. Nevertheless, initial investigations seem to be promising. MNs obtained through differentiation of iPSCs have been shown to possess numerous characteristics of bona fide MNs, including distinctive electrophysiological responses and the ability to form functional neuromuscular junctions (NMJs) (101). Moreover, it was reported that iPSC-derived MNs of ALS patients recapitulate key aspects of the adult human pathology (13).

The first reports that described a pathological phenotype in iPSC-derived MNs from ALS patients were published in 2012. Bilican *et al*. and Egawa *et al*. were able to recapitulate aspects of TDP-43 proteinopathy in iPSC-derived MNs carrying a TDP-43 mutation (106,107). In addition to cytosolic TDP-43 aggregation, it was observed that these MNs showed a selective vulnerability to cell stressors (106,107). TDP-43 aggregates (in this case intranuclear) were also found in a subset of sporadic ALS iPSC-derived MNs (108). Similar findings have been found in iPSCs derived from patients carrying the hexanucleotide expansion in the *C9ORF72* gene. Almeida *et al*. and Donnelly *et al*. observed the presence of RNA foci containing GGGGCC repeats and RAN translation products in iPSC-derived neurons (109,110). Increased susceptibility to cellular stress due to inhibition of autophagy (109) and to glutamate excitotoxicity (110) was also observed. Interestingly, Donnelly *et al*. observed global

alterations in RNA metabolism in patient iPSC-derived MNs, which could be reverted by anti-sense oligonucleotides targeting *C9ORF72* mRNA (110). This demonstrates the potential of iPSCs for screening drug candidates. Furthermore, iPSC-derived MNs have been created from patients with mutations in SOD1 (111). These MNs developed neurofilament inclusions as an early pathological event (111), which has also been observed in transgenic mSOD1 mouse models (112). The presence of neurofilament inclusions in the iPSC-derived MNs indicates the misregulation of neurofilaments, which results in axonal transport pathology. This is in line with the observed retraction of axonal terminals and denervation of muscles before the loss of cell bodies (111). Wainger *et al*. demonstrated that iPSC-derived MNs from ALS patients carrying mutations in the *SOD1*, *C9ORF72* or *FUS* gene all showed membrane hyperexcitability, which is also a characteristic feature of ALS (113). Very recently, cytoplasmic mislocalization of the FUS protein was also replicated in FUS-ALS iPSC-derived MNs (114). The authors showed that severity of FUS mislocalization and cellular vulnerability was determined by the underlying FUS mutation and neuronal aging (114). The co-localization of FUS within stress granules has also been shown in iPSC-derived MNs after they were subjected to cellular stress (115).

Taken together, these studies indicate that iPSC-derived MNs from ALS patients resemble **early stages of the disease** and they support the occurrence of an intrinsic vulnerability to stress (116). The use of iPSCs appears to be a **promising opportunity to develop a human cellular model for ALS**, avoiding the use of transgenic overexpression of mutant ALS genes and in a human genetic background.

Chapter 2: Objectives

ALS is characterized by the degeneration of motor neurons resulting in a loss of motor function. A better understanding of early disease mechanisms is needed to create new therapeutic strategies. Mutations in the DNA/RNA binding protein **FUS** is one of the genetic causes of ALS. Although mutations in the NLS of FUS often lead to a cytosolic mislocalization of the protein, the way in which impaired nuclear import of FUS mediates neurodegeneration remains to be elucidated. In addition, it is hypothesized that a decrease in **axonal transport** is an early event in the pathogenesis of ALS (63). To gain insight into the pathological mechanisms of ALS, I studied the impact of ALS causing genetic defects (FUS mutations) on axonal transport. To overcome the inability to obtain patient diseased tissue, I made use of MNs differentiated from iPSCs derived from ALS patients harboring a FUS mutation. To date, no studies investigating axonal transport in FUS-ALS patient iPSC-derived MNs have been reported.

This thesis has two aims:

1) **Generation and characterization of iPSC-derived motor neurons** obtained from FUS-ALS patients and healthy controls. The first part of my thesis exists of characterizing the differentiated neurons and of confirming the formation of MNs. Because ALS is an adult onset disease our hypothesis is that control and patient cell lines will differentiate with similar efficacy into MNs.
2) **Investigating** whether **ALS-specific phenotypes** are present in patient-derived MNs. We hypothesized that the iPSC-derived MNs could recapitulate early features observed in FUS-ALS patients such as FUS cytoplasmic mislocalization.

Chapter 3: Materials and methods

Human iPSC lines

The human iPSC-lines used in this study are listed in Table 1. Fibroblasts from a 71-year-old female ALS patient which is a carrier of the R521H FUS mutation (family history of ALS), a 17-year-old male ALS patient carrying the *de novo* P525L FUS mutation (parents negative for the mutation) and two healthy controls without FUS mutation (male, age at biopsy 50; female, age at biopsy 49) were reprogrammed using non-integrating Sendai virus expressing the reprogramming factors *Oct4*, *Sox2*, *c-Myc* and *Klf4* (CytoTune®-iPS 2.0 Sendai Reprogramming Kit, Invitrogen) to establish the iPSC lines: FUS R521H, FUS P525L, WT1 and WT2, respectively. The healthy controls are family members of the 17-year-old ALS patient (coded FUS P525L), namely the father and mother respectively. There is no consanguinity with the first mentioned ALS patient. The human iPSC lines were cultured on Geltrex (Gibco) and kept in culture in Essential 8 medium (Gibco). To confirm the presence of mutations in the obtained iPSC lines, DNA was collected by using a DNA extraction kit (QAIGEN) and sequenced by the company IDT (Munich, Germany). The following primers were used: forward: 5' CATTTTGAGGGCTAGGTGGA 3' and reverse 5' AGTGAAAAGGGGGAAGAGGA 3'. All procedures were in accordance with the Helsinki convention and approved by the Ethical Committee of the KU Leuven (Nr. ML 4073).

Code	Diagnosis	Gender	Mutation	Age at biopsy (years)	Disease duration (months)
FUS R521H	FALS	F	R521H	71	29
FUS P525L	FALS	M	P525L	17	15
WT1	Healthy control	M	/	50	/
WT2	Healthy control	F	/	49	/

Table 1. Human iPSC lines. F= Female, M= Male, WT= Wild type.

Motor neuron differentiation

MN differentiation was performed as described before (117) with some small modifications. Human iPSCs were dissociated with collagenase type IV (Gibco) and transferred to ultra low attachment T25 flasks at day 0. MN differentiation was performed by cultivation of the cells in differentiation medium N2B27 (Dulbecco's Modified Eagle Medium (DMEM) F12, Neurobasal vol:vol, supplemented with N2 supplement (Life technologies), B27 supplement without vitamine A (Life technologies), Pen-strep 1% (Gibco), β-mercapto-ethanol 0.1% (β-ME; Life technologies), ascorbic acid (0.5 µM, Sigma-Aldrich)) supplemented with different components at indicated time points and indicated

concentrations (Fig. 5). Neuralization of iPSCs was initiated by cultivation of the cells supplemented with Y-27632 (5µM, Calbiochem), SB431542 (40 µM, Tocris), CHIR99021 (3µM, Tocris) and LDN 193189 (0.2µM, Stemgent) for two days. At day 2 retinoic acid (RA, 100nM, Sigma-Aldrich) and Smoothened Agonist (SAG, 500nM, Calbiochem) were added to the medium to induce caudalization and ventralization of the neuroepithelial stem cells (NEPs). This medium was changed every 2-3 days till day 6. At day 7, brain derived neurotrophic factor (BDNF, 10 ng/ml, PeproTech) and glial cell derived neurotrophic factor (GDNF, 10 ng/ml, PeproTech) were added to the medium. At day 9, DAPT (indicated concentrations, Tocris) was supplemented to the differentiation medium N2B27 for terminal differentiation. The medium was changed every 2-3 days. At day 10, the embryonic bodies were dissociated using trypsin and $0.5x10^5$ or $1\text{-}2x10^5$ cells were seeded in a poly-L-ornitine (100µg/ml, Sigma) and laminin (20 µg/ml, Life technologies) coated 12-well plates for axonal transport and immunostaining, respectively. From day 14, RA and SAG were removed from the medium. Ciliary neurotrophic factor (CNTF, 10 ng/ml, Propotech) was added to the differentiation medium N2B27 at day 16. After terminal differentiation (day 17) DAPT was removed from the medium and cells were maintained for up to 32 days for further maturation in neuronal medium supplemented with BDNF, GDNF and CNTF. The medium was changed every 2-3 days.

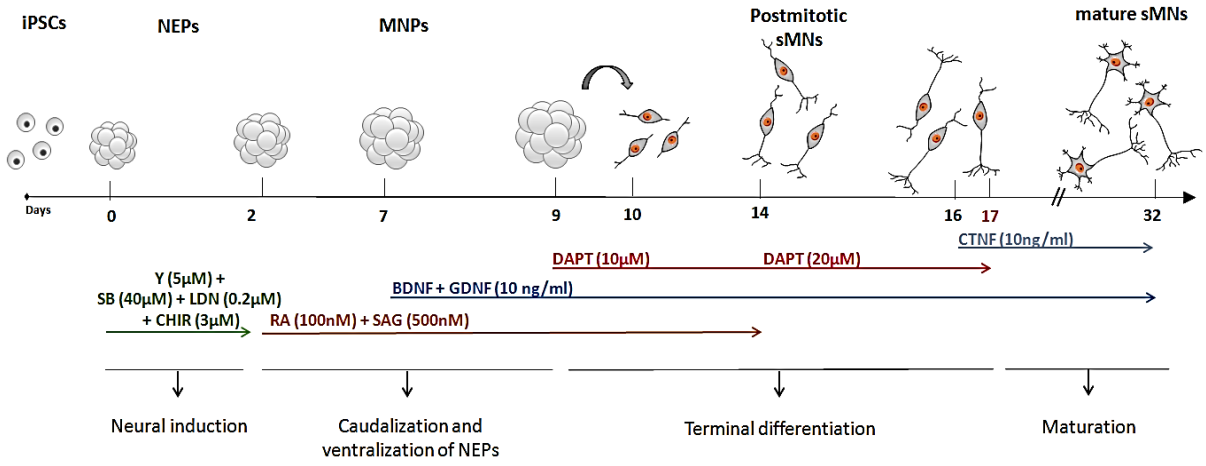

Figure 5. Schematic representation of the MN differentiation protocol. iPSCs= induced pluripotent stem cells; NEPs= neuroepithelial stem cells; MNPs= motor neuron progenitors; sMNs= spinal motor neurons; RA= retinoic acid; SAG= Smoothened Agonist; BDNF= brain derived neurotrophic factor; GDNF= glial cell derived neurotrophic factor; CNTF= ciliary neurotrophic factor. Figure is based on information in the review of Davis-Dusenbery *et al*. (2014) (101) and Sances *et al*. (2016) (103).

Immunostaining

Cells were washed once with phosphate buffer saline (PBS), fixed with 4% paraformaldehyde (20 min at room temperature) and rinsed again 3 times with PBS. 5 % normal donkey serum (NDS, Sigma) in 0.1% Triton X-100 in PBS was used for blocking at room temperature for 1 hour. Primary antibodies

were diluted in 2% NDS in 0.1% PBS Triton and incubated overnight at 4°C. The primary antibodies: rabbit anti-Oct3/4 (Santa Cruz biotechnologies; 1:400), goat anti-Nanog (R&D; 1:500), mouse anti-SSEA4 (Santa Cruz Biotechnologies; 1:200) and mouse anti-Tra-1-60 (Millipore; 1:1000) were used as markers to analyze pluripotency capability of the iPSC lines. The primary antibodies: goat anti-Hb9 (homeobox transcription factor, Santa Cruz Biotechnologies, 1:50), mouse anti-βIII-tubulin (βIII-Tub., Abcam, 1:1000), rabbit anti-Isl1 (insulin gene enhancer protein1, Millipore; 1:200), mouse anti-Smi32 (Covance, 1:500), rabbit anti-Chat (Choline acetyltransferase, Life technologies; 1:200) were used for MN characterization. The primary antibodies rabbit anti-FUS (Proteintech; 1/100) and mouse anti-βIII-tubulin (Abcam, 1:1000) were used to analyze FUS cytoplasmic mislocalization. Secondary antibodies were added for 3 hours at room temperature. The secondary antibodies: alexa 488/555 goat anti-rabbit and alexa 488/555 goat anti-mouse and alexa 488/555 donkey anti-goat (Life Technologies; 1:2500) were used. Prolong gold anti-fade reagent with 4',6-diamidino-2-phenylindole (DAPI) was used for moanting (Life Technologies). Images were taken with the microscope Zeiss Image M1 with visible excitation lines at 405, 488 and 555 nm.

Mitotracker/lysotracker loading and life imaging

At day 32, iPSC-derived MNs were incubated at 37 °C with 50 nM MitoTracker Red FM (Invitrogen) for 20 minutes or 50 nM LysoTracker Red DND-99 (Invitrogen) for 1 hour and left them to equilibrate (min 30 min) in their original differentiation medium. All experiments were performed during constant perfusion of warm 36 ± 0.5 °C HEPES buffered salt solution (pH= 7.4, composition in mM: 150 NaCl, 5 KCl, 1 $MgCl_2$, 2 $CaCl_2$, 10 glucose, 10 HEPES). Mitochondrial/lysosomal movements were recorded for 200 sec with one-second time-lapse intervals using an inverted Zeiss Axiovert 200M microscope (Carl Zeiss) with a 40x water immersion lens. Mitrotracker-RED FM and LysoTracker Red DND-99 were excited at 581 nm with an exposure time of 20 ms and at 577 nm with an exposure time of 30 ms, respectively, using a TILL Poly V light source (TILL Photonics). All videos were taken within a 30 minute range after the setup.

Transport analysis

All image analysis were performed in Igor Pro (Wavemetrics) using custom-written routines. Neurites were manually tracked starting from the most proximal point that is closest to the cell body until they were no longer visible or no longer able to track. Neurites were selected blindly when possible and based on their capacity to be analyzed. The axon was chosen when it was distinguishable (defined as the longest neurite). Kymographs were constructed for each video. The following parameters were extracted from these graphs: number of moving mitochondria/lysosomes

(manually); number of bidirectional, retrograde and anterograde moving lysosomes (manually); stationary mitochondria/lysosomes (automatically), length of the neurite/farthest-reaching lysosome (automatically based on following command: print dimsize(M_Imagelineprofile,0)*.323). As a general rule, mitochondria are considered to be stationary if they remain immobile for the entire recording period. A mobile mitochondria is counted only if its displacement is at least 5 µm during the same period (118). No difference was made between movements that covered a big or a small distance. This data was then exported to Microsoft Excel to calculate the total number of mitochondria/lysosomes per 100µm, number of moving mitochondria per 100 µm, the percentage of moving mitochondria/lysosomes and the percentage of bidirectional, retrograde and anterograde moving lysosomes.

Patch-clamp recordings

Whole-cell current-clamp and voltage-clamp measurements were carried out by using an EPC-10 amplifier and Patchmaster software (HEK Elektronik). Pipette electrodes were fabricated and fire polished with a final tip resistance of 2-5M. Recordings were performed at room temperature and the iPSC-derived MNs were superfused with external solution consisting of (in mM): 140 NaCl, 5 KCl, 2 $CaCl_2$, 2 $MgCl_2$, 10 Hepes and 12 glucose. The pipette solution contained (in mM): 120 K-gluconate, 20 KCl, 1 $MgCl_2$, 10 Hepes, 0.2 EGTA, 0.3 Na-GTP, 5 NaCl and 4 Mg-ATP. In voltage clamp measurements, the holding potential was -70mV, if not mentioned otherwise. Patch-clamp recordings were performed in co-operation with Dr. Ann Swijsen of the neurobiology lab.

Statistics

Statistical analysis were performed using GraphPad Prism. A One-way ANOVA or Kruskall-Wallis test followed by an unpaired t-test or Mann-Whitney test was used for statistical analysis. Shapiro-Wilk normality test was used. The data are presented as mean $\pm$ SD.

Chapter 4: Results

4.1. iPSC-derived motor neuron generation and characterization

4.1.1 Generation of iPSCs

iPSCs were previously generated from fibroblasts of two ALS patients harbouring a mutation in the NLS domain of FUS (R521H, P525L) and two healthy controls (wild-type (WT) FUS) by expressing the reprogramming factors *Oct4*, *Sox2*, *c-Myc* and *Klf4*. In order to model the disease successfully, the maintenance of FUS mutations after reprogramming is essential. Sequencing confirmed the maintenance of point mutations R521H and P525L in patient-derived iPSC lines and the absence of mutations in control cell lines (Fig. 6). Both the ALS and WT iPSC colonies exhibited typical morphology and expressed the pluripotency markers Nanog, Oct3/4, SSEA-4 and Tra1-60 (Fig. 7).

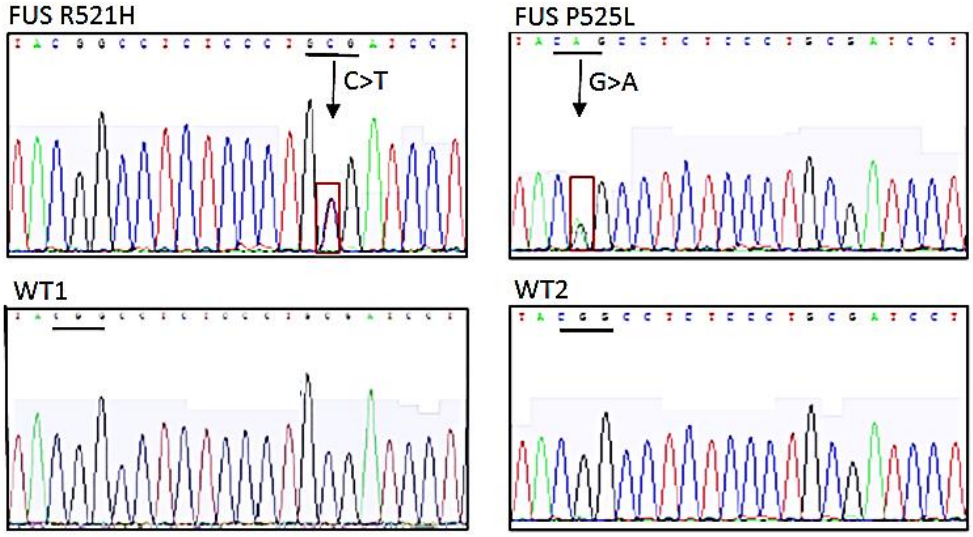

Figure 6. Sequencing results of the FUS gene in iPSC lines. DNA sequencing confirmed the presence of heterozygous mutations R521H (c.C2562T) and P525L (c.G1574A) in the patient iPSC lines. Sequencing of the FUS gene in control iPSC lines (WT1, WT2) did not reveal mutations. Mutations are indicated by arrows.

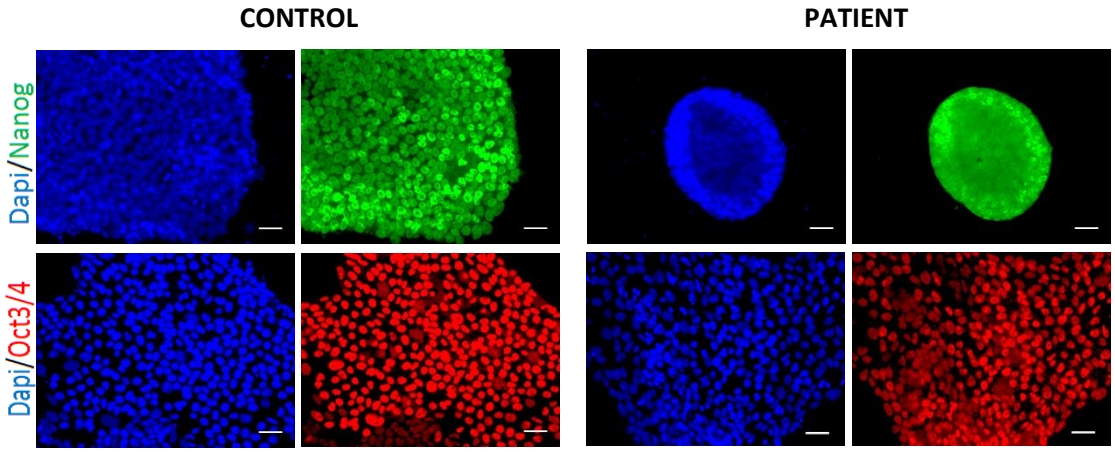

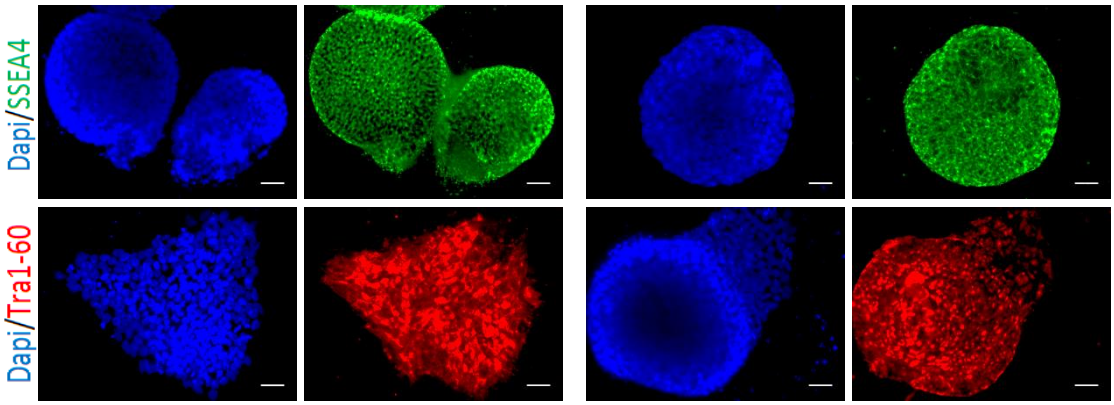

Figure 7. iPSC cultures expressing pluripotency markers Nanog, Oct3/4, SSEA4 and Tra1-60. Representative images for control (WT2) and patient (FUS P525L) cell lines are shown. Scale bar= 40 µm.

4.1.2 Motor neuron differentiation of control and ALS iPSC lines

In order to compare MNs from healthy controls and ALS patients, the iPSC lines were differentiated in parallel into MNs (Fig. 8). MN differentiation was done according to the differentiation protocol shown in figure 5. Serial and overlapping developmental steps that mimic MN development *in vivo* were followed. First, human iPSCs were differentiated to NEPs through dual SMAD inhibition (LDN and SB) and Wnt activation (CHIR). Subsequently, caudalization is induced by RA signalling (spinal cord identity), followed by the induction of ventralization though a combined action of RA and SAG signalling (MN identity). During these first steps the cells were cultured on low-attachment flasks and formed EBs (Fig. 8). After 9 days of differentiation, EBs were dissociated and plated on poly-L-ornithine/laminin coated coverslips. DAPT, a γ-secretase inhibitor, was added to the differentiation medium to induce conversion of spinal MN progenitors into post-mitotic spinal MNs (terminal differentiation) (Fig. 8). MN differentiation ended at day 17. The immature MNs were kept in culture for further maturation in neuronal medium supplemented with the neurotrophic factors BDNF, GDNF and CNTF, until day 32. At 32 days of neuronal differentiation, cells were clustered together in small colonies and a dense network of neurites was formed (Fig. 8). iPSC lines harbouring a FUS mutation that were subjected to the MN differentiation protocol produced populations of MNs with similar morphology as control iPSCs lines (Fig. 8-9). Using immunostaining for cytoskeletal markers neurofilament light (NFL) and βIII-tubulin a typical MN morphology was observed, which includes a multipolar neuronal morphology with a long axon (Fig.9).

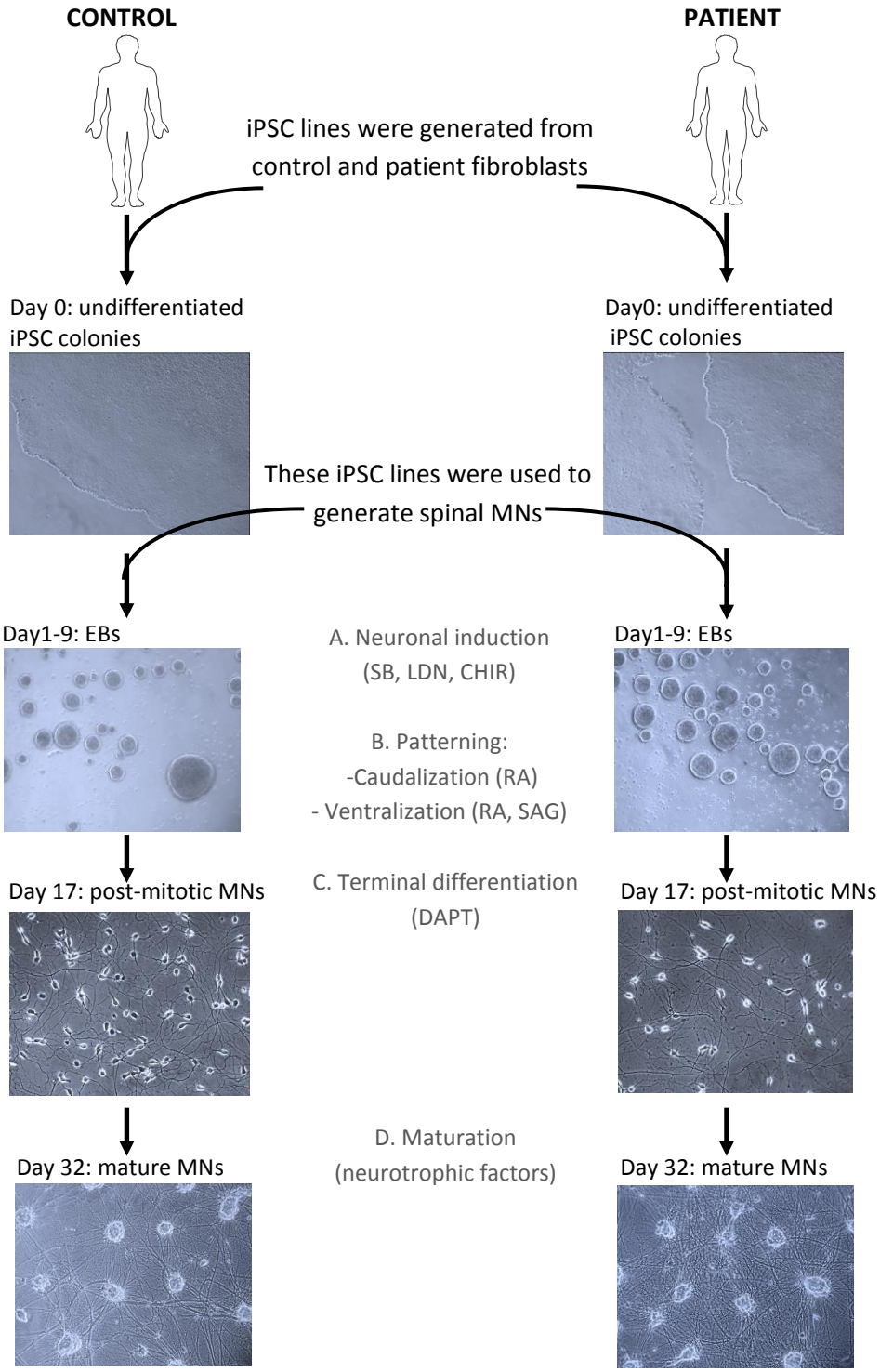

Figure 8. **Differentiation of iPSCs into spinal MNs.** Representative bright-field images for control (WT2) and patient (FUS P525L) cell lines are shown. Cell lines were differentiated in parallel**.** During the first two days of the differentiation process, cells were exposed to 40 µM SB, 0.2µM LDN and 3µM CHIR to induce neuronal induction. Subsequently, spinal cord and MN identity was induced in the presence of 0.1 µM RA and 500 nM SAG. Cells were cultured on low-attachment flasks to form EBs. After 9 days of differentiation, EBs were dissociated and plated on poly-L-ornithine/laminin coated coverslips. DAPT induced terminal differentiation. MNs were kept in culture for further maturation in neuronal medium supplemented with BDNF, GDNF and CNTF, until day 32. iPSC= induced pluripotent stem cell, EBs= embryonic bodies; MNs= motor neurons; RA=retinoic acid; SAG= smoothened agonist. Magnification: 10x (iPSC culture, EBs, mature MNs), fourth image); 20x (post-mitotic MNs)

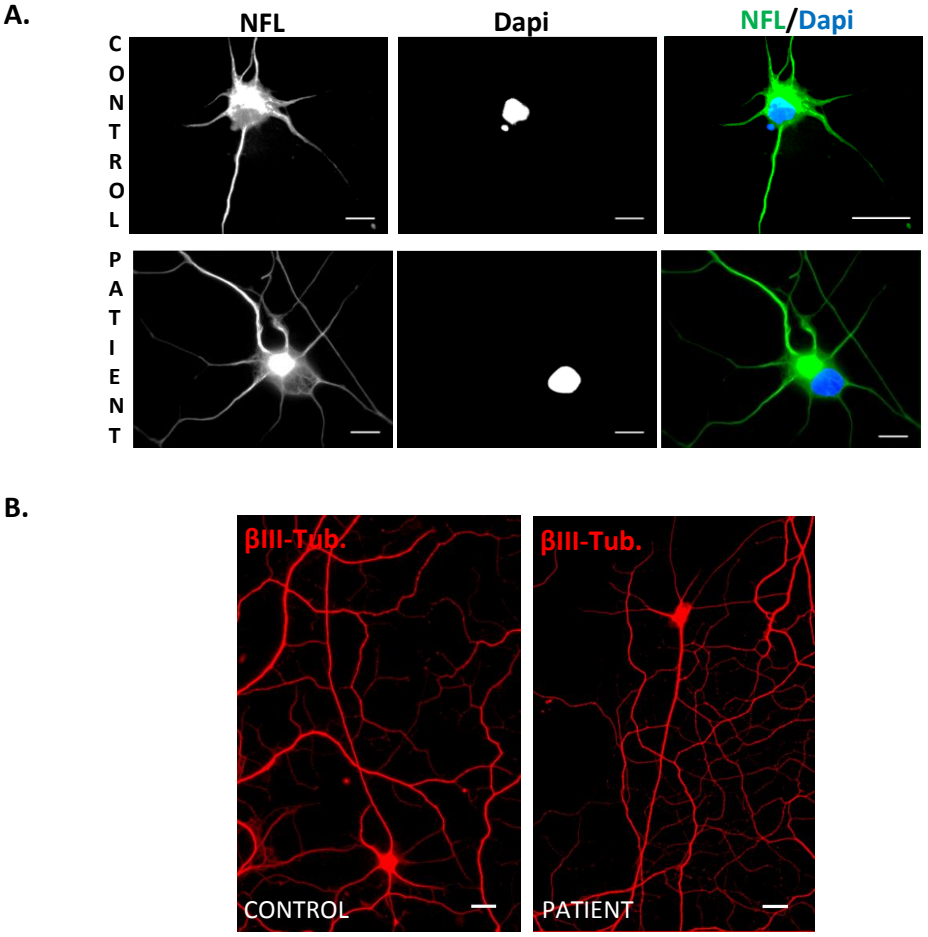

Figure 9. Immunostaining showed multipolar neuronal morphology with a long axon at day 32. NFL= neurofilament light. βIII-tub.= βIII-tubulin. Representative images for control (WT2) patient (FUS P525L) cell lines are shown. (A) Scale bare= 10 µm. (B) Scale bare=20 µm.

4.1.3 Both control and ALS patient iPSCs have the potential to differentiate into motor neurons with high efficacy

To further identify whether *FUS* mutations affect MN generation *in vitro*, immunostaining was performed to characterize the differentiated neurons. This includes the embryonic MN marker Hb9 and the mature MN markers insulin gene enhancer1 (Isl1), Smi32 and choline acetyl transferase (Chat) (Fig. 10). Hb9-positive neurons were observed at day 17 of the differentiation protocol, but no longer at day 32 (Fig. 10A). Both control and patient cell lines co-expressed on day 17 (end of MN differentiation) and still on day 32 (after maturation) the mature MN markers Isl1 and Smi32 (Fig. 10B). Smi32 stains neurofilament heavy chain and was present in the cell body and neurites of the differentiated neurons. Isl1 is a MN-specific transcription factor and was observed in the nucleus of the differentiated cells. More than 70 % of the differentiated cells were positive for Isl1 at the end of the differentiation protocol (Fig. 11 control: 73.8 $\pm$ 7.4%; patient: 78.5 $\pm$ 7.9%), suggesting a high differentiation efficacy. There was no significant difference between control and ALS patients. Also Chat, which is characteristic for a cholinergic MN phenotype, was expressed in both patient and

control cell lines on day 17 and on day 32, with a stronger expression after maturation (day 32) (Fig. 10C).

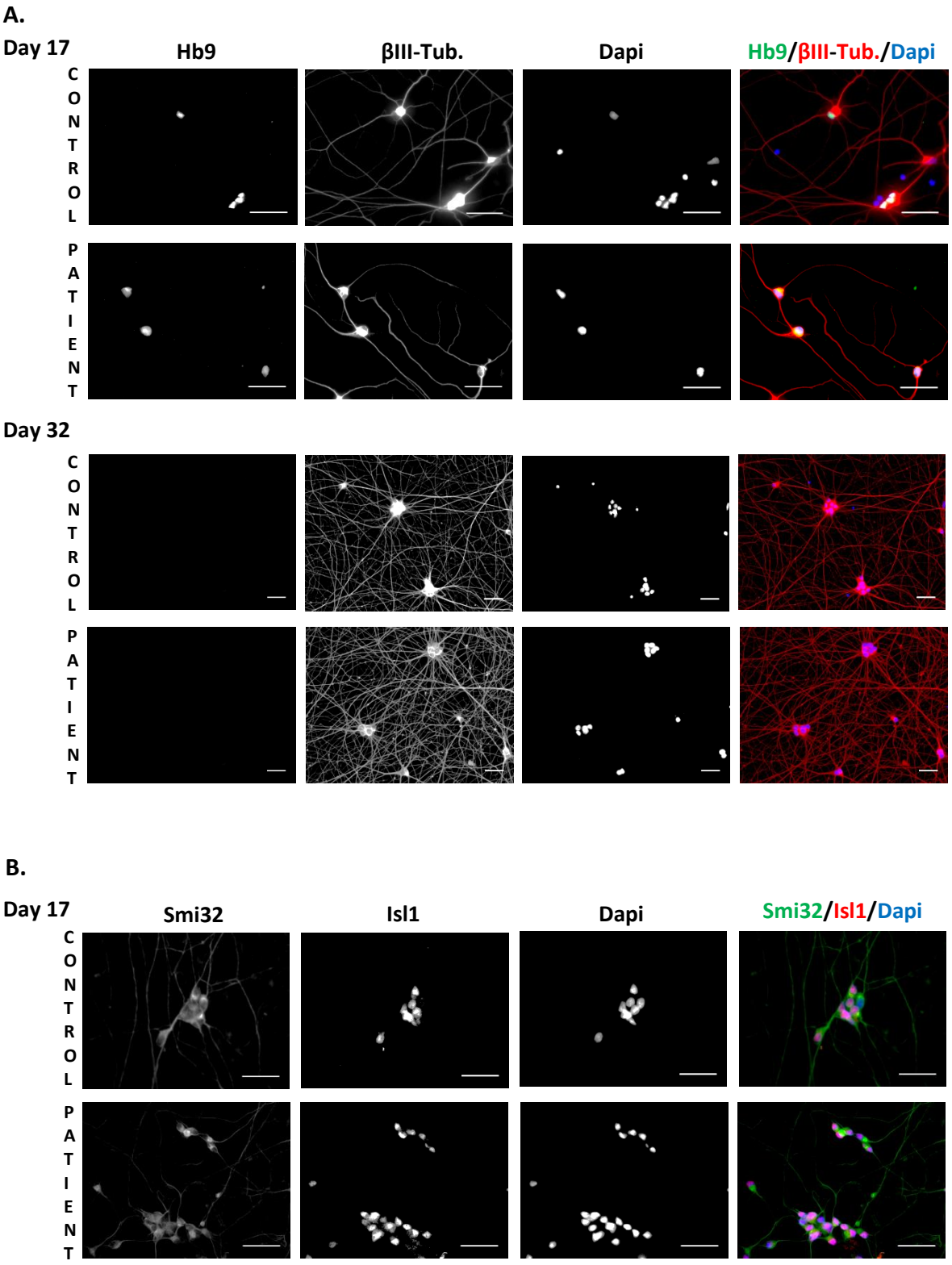

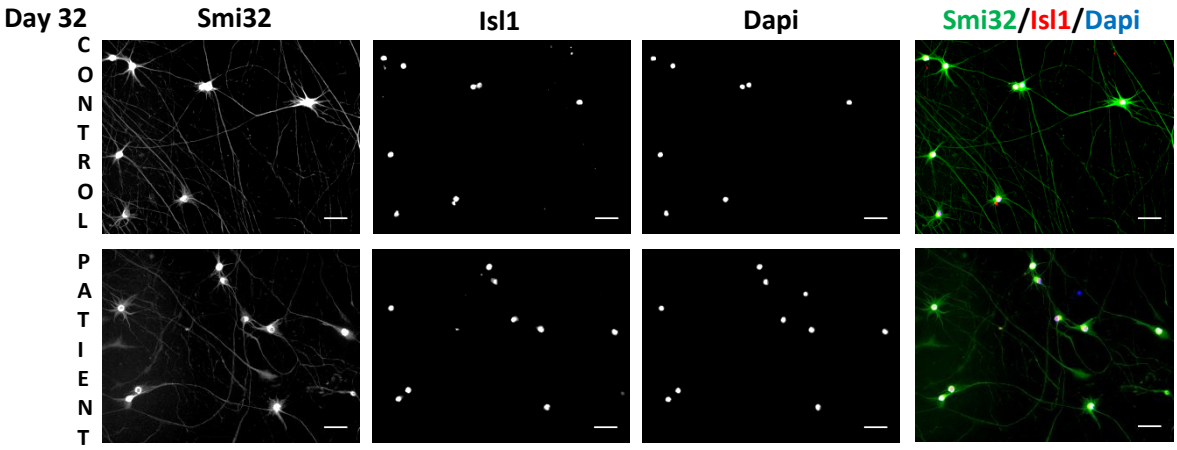

C.

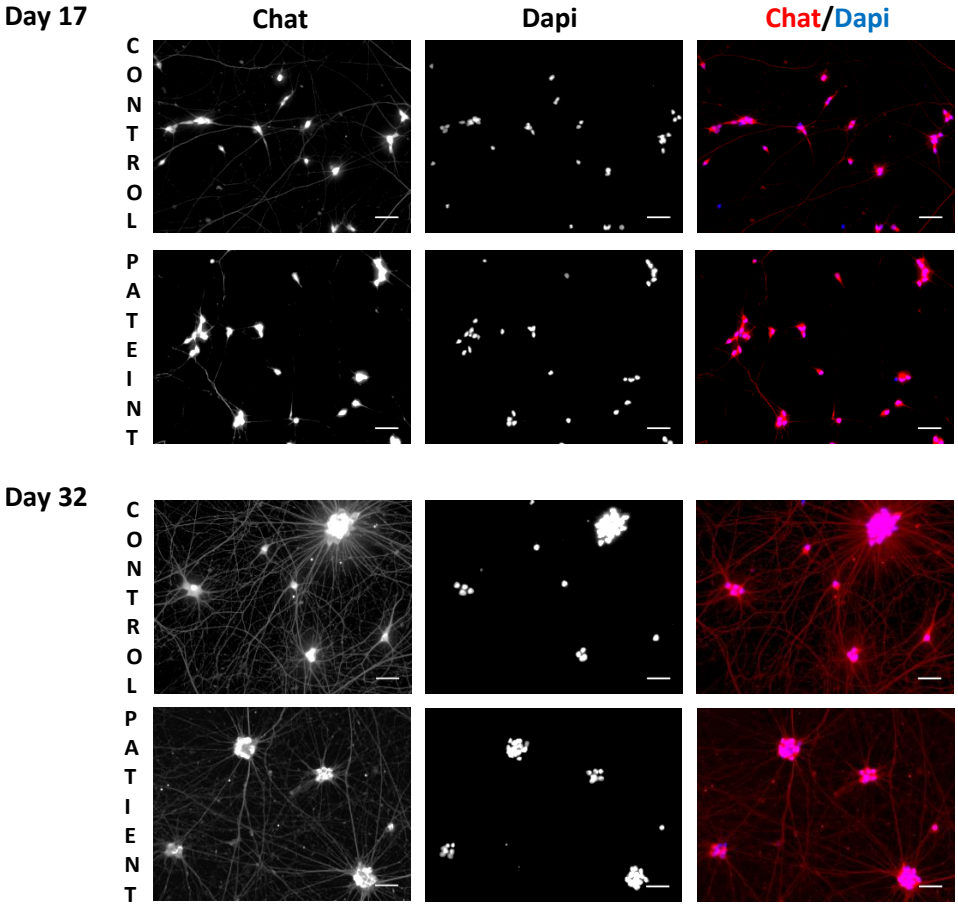

Figure 10. Immunocytochemical characterization of iPSCs derived motor neurons. Characterization of differentiated MNs included **(A)** the pan-neuronal and cytoskeletal marker βIII-Tubulin (βIII-Tub.) and the embryonic MN marker Hb9, **(B)** the mature MN markers Isl1 and Smi32 and **(C)** Choline acetyl transferase (Chat). Day 17 (end of MN differentiation) and day 32 (after maturation) are shown. Representative images for control (WT2) and patient (FUS P525L) cell lines are shown. Scale bar = 40 µm.

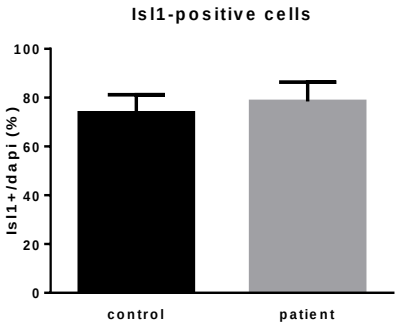

Figure 11. Percentage of Isl1 positive cells at day 17. Representative data for both control (WT2) and patient (FUS P525L) cell lines are shown. Mean ± SD is shown. Control: n =249. Patient: n = 616.

Although the expression of canonical MN markers has been shown to be reliable indicators of MN characteristics, when used alone it is insufficient to evaluate the success of differentiation. Therefore, electrophysiological activity was analyzed to investigate functionality of the differentiated MNs after maturation (day 32) (Fig. 12). Voltage clamps recordings showed that the MNs of both patient and control cell lines can fire action potentials in response to current injections (Fig. 12A) and express functional voltage-dependent Na^+ and K^+ channels (Fig. 12C). Moreover, the iPSC-derived MNs displayed a spontaneous and repetitive action potential firing that is characteristic for functional maturation (Fig. 12B) and displayed spontaneous postsynaptic currents (Fig. 12D), indicating functional synapse formation between neurons. Patch-clamp recordings were performed by Dr. Ann Swijsen (Laboratory of Neurobiology). These data implicate that mature and functional MNs can be differentiated from FUS-ALS patient specific iPSCs and that the initial development is not altered through FUS mutations.

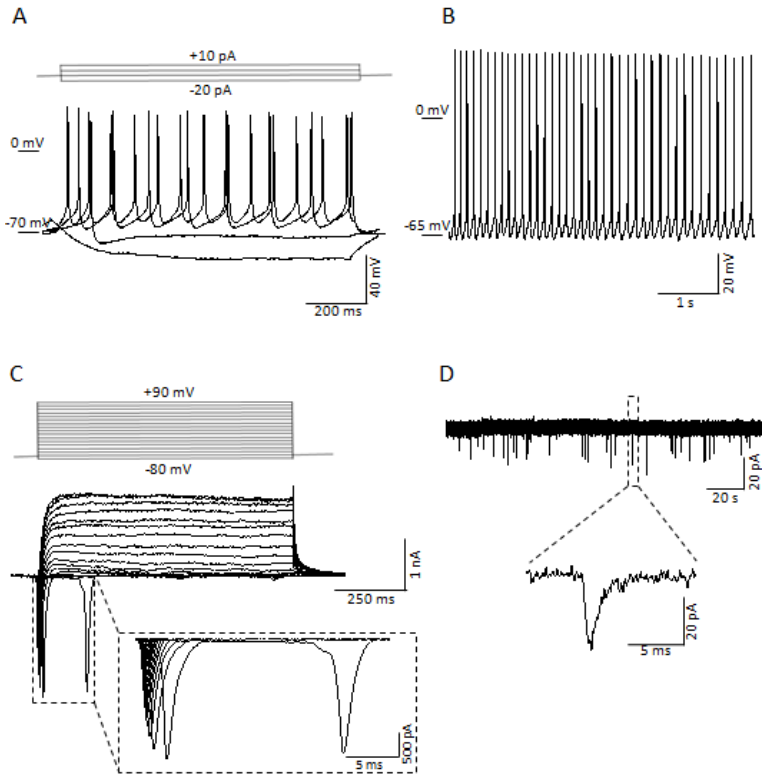

Figure 12. Electrophysiological activity of iPSC-derived MNs at day 32. (A) Evoked action potential. Experimental current pulse step protocol (top panel) and representative traces of membrane potential responses to current injections (lower panel). The membrane potential was current-clamped at approximately -70 mV between current pulses. **(B) Spontaneous action potentials.** Representative recording of spontaneous action potentials. No current injection was applied. **(C) Voltage-gated channels.** Experimental voltage pulse step protocol (top panel) and representative traces of current responses showing voltage-activated inward (expanded in dashed box) and outward currents. **(D)** Recording of **spontaneous postsynaptic currents** recorded at a membrane holding potential of -70 mV. Representative graphs are shown.

4.2 ALS-phenotype characterization

4.2.1 Cytoplasmic mislocalization of FUS in iPSC-derived MNs from ALS patients harbouring a FUS mutation

In the second part of my thesis I investigated whether FUS-ALS associated phenotypes were present in patient iPSC-derived MNs. Our patient cell lines were obtained from two ALS patients with mutations in the NLS of FUS (R521H, P525L). These kind of mutations have been shown to cause FUS cytoplasmic mislocalization (17,49). As a consequence, the intracellular localization of FUS was visualised using immunostaining in primary fibroblasts, undifferentiated iPSC colonies and iPSC-derived MNs from both ALS patients and healthy controls (Fig. 13-15). Fibroblasts from the two healthy individuals (WT1 and WT2) showed FUS-staining mainly in the nucleus (Fig. 13). Fibroblasts with a decreased staining in the nucleus were observed in both of the patient cell lines (P525L, R521H) (Fig. 13), indicating cytoplasmic mislocalization of mutant FUS. Moreover, the frequency of FUS cytoplasmic mislocalization was mutation dependent. In the majority of fibroblasts expressing FUS P525L a decreased nuclear localization of FUS could be observed. In contrast, nuclear localization of R521H FUS was only decreased in some single cells. In undifferentiated iPSC colonies, FUS cytoplasmic mislocalization could strongly be detected within the P525L mutant cell line (Fig. 13). In contrast, an enhanced cytoplasmic localization of R521H FUS was only rarely observed (Fig. 13). Concerning iPSC-derived MNs, FUS was predominantly expressed in the nuclei of neurons in both mutant cell lines. However, there was some FUS diffusely present in the neurites, both at the end of the MN differentiation (Fig. 14) and after maturation (Fig. 15). In control cells only a low amount of FUS could be detected in the neurites (Fig. 14-15), indicating some FUS cytoplasmic mislocalization in patient-derived MNs. In line with the fibroblasts and undifferentiated iPSC cultures, iPSC-derived MNs expressing the P525L mutation showed a stronger cytosolic mislocalization of FUS, in comparison to R521H FUS (Fig. 15).

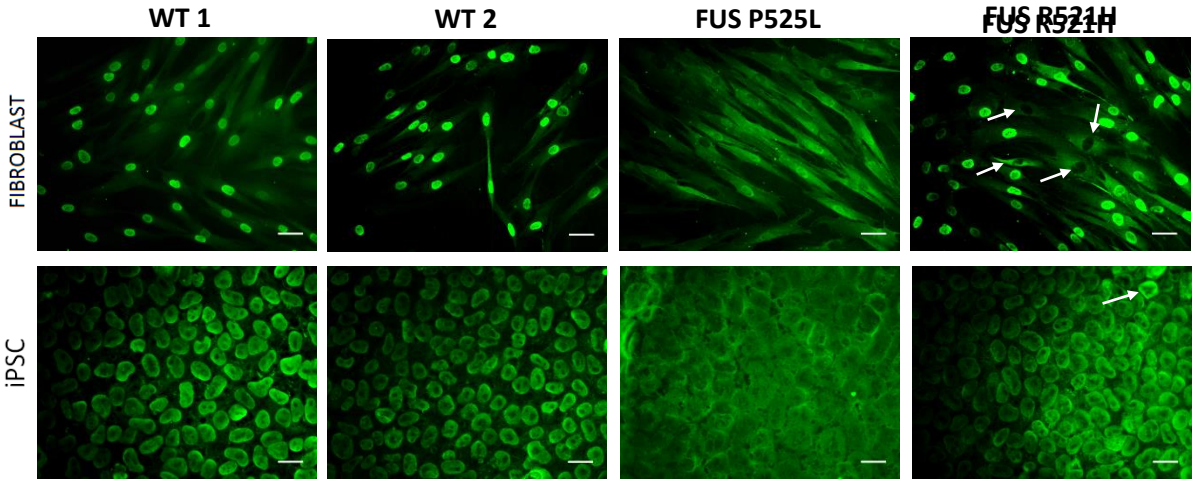

Figure 13. Cytoplasmic mislocalization of mutant FUS. Immunostaining showing intracellular localisation of WT and mutant FUS protein in fibroblasts and iPSC colonies. **(Fibroblasts)** WT FUS protein was mostly distributed in the nucleus, only a small proportion was distributed in the cytoplasm. P525L FUS show cytoplasmic mislocalization in the majority of cells. R521H FUS was mislocalized to the cytoplasm in single cells (arrows). **(iPSC colonies)** WT FUS was distributed in the nucleus of undifferentiated iPSC colonies. Cells carrying the P525L mutations displayed a strong cytoplasmic mislocalization in every cell. Mislocalization of R521H was rarely observed (arrow). Scale bar fibroblasts= 40 µm; Scale bar iPSCs= 20 µm.

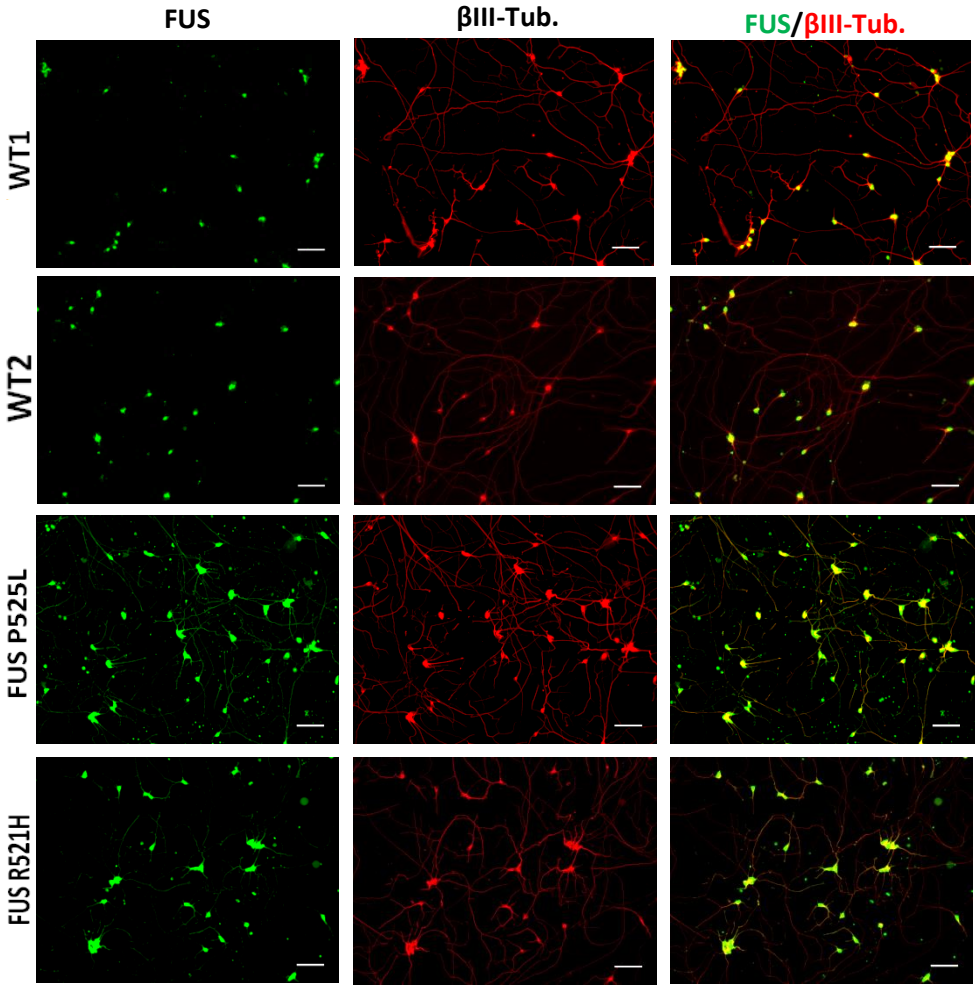

Figure 14. Cytoplasmic mislocalization of mutant FUS. Immunostaining showing intracellular localisation of WT and mutant FUS protein in iPSC-derived MNs at the end of the MN differentiation (day 17). Staining of FUS in the neurites of iPSC-derived MNs was higher in patient cell lines in comparison to control cell lines, indicating FUS cytoplasmic mislocalization. Scale bar= 40 µm.

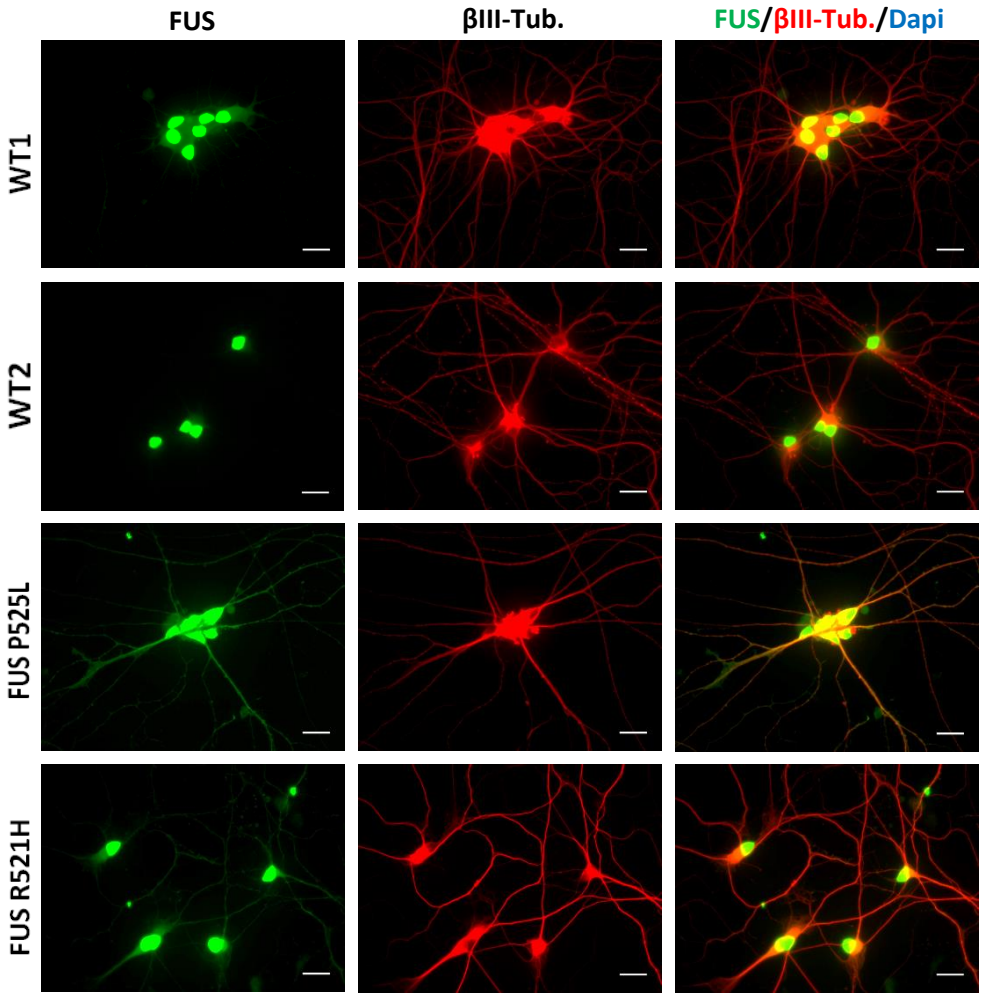

Figure 15. Cytoplasmic mislocalization of mutant FUS. Immunostaining showing intracellular localisation of WT and mutant FUS protein in mature iPSC-derived MNs (day32). Staining of FUS in the neurites of iPSC-derived MNs was higher in patient cell lines in comparison to control cell lines, indicating FUS cytoplasmic mislocalization. Scale bar= 20 µm.

4.2.2 iPSC-derived motor neurons of ALS patients harbouring a FUS mutation exhibited reduced mitochondrial transport

Disturbances of mitochondrial transport are implicated as an early event in the pathogenesis of ALS. Therefore, we assessed mitochondrial transport in iPSC-derived mature MNs cultures in both patient and control cell lines. Using a selective mitochondrial marker (MitoTracker-RED) mitochondria were analyzed in day 32 iPSC-derived MNs with time-lapse imaging. The movies were converted into kymographs to quantify total and moving mitochondria (Fig. 16). In these maps, mitochondria with no displacement during the time elapsed are indicated as vertical lines (stationary mitochondria).

Diagonal lines represent moving mitochondria and their direction can be determined. Calculations of the percentage of motile mitochondria revealed a significant reduction in ALS iPSC-derived MNs compared to WT MNs (Fig. 17A. WT1= 14.1 ± 6.1%; WT2= 23.8 ± 12.7%; FUS P525L= 8.9 ± 3.3%; FUS R521H=8.9 ± 4.4%). In addition, MNs derived from ALS-patients harbouring a FUS mutation showed a reduction in the number of total mitochondria (moving + stationary) (Fig. 17B; number per 100 µm: WT1= 19.0 ± 2.3; WT2= 18.1 ± 1.8; FUS P525L= 16.6 ± 3.5; FUS R521H= 15.4 ± 3.0). These two observations are confirmed by the observation that also the absolute number of moving mitochondria in ALS-patients derived MNs was significantly decreased in comparison to control-derived MNs (Fig. 17C; Number per 100 µm: WT1= 2.4 ± 1.1; WT2= 3.3 ± 1.2; FUS P525L= 1.5 ± 0.8; FUS R521H= 1.3 ± 0.6). The observed reduction in percentage and number of moving mitochondria was confirmed in two extra independent experiments (supplementary data Fig. 1A-B). The reduction in total number of mitochondria is a less strict finding because it was only observed in one of the two repeated experiments (supplementary data Fig. 1A-B). These results suggest that mitochondrial transport is impaired in the MNs obtained from the ALS patients. Remarkably, in one of the experiments no significant differences could be observed between patient and control-derived MNs in either percentage of moving mitochondria, total mitochondria and number of moving mitochondria (Fig. 18). A major difference in this experiment was the presence of a large amount of glial cells, which could be astrocytes based on their morphology (Fig. 19). Future experiments will have to be performed to investigate whether the presence of these glial cells could explain the difference in the observed phenotype.

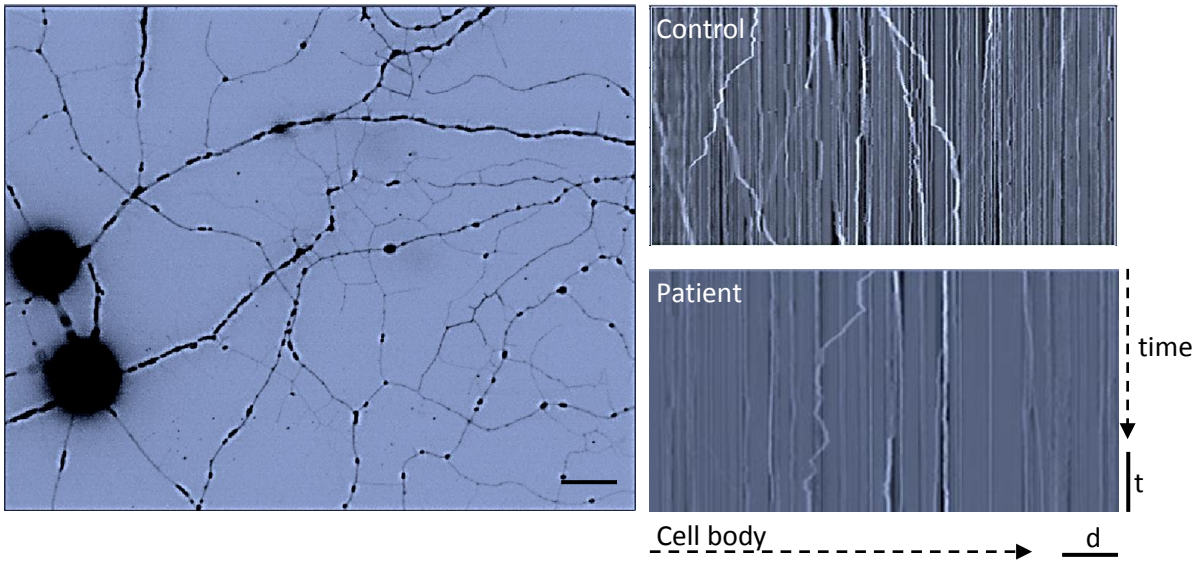

Figure 16. Mitochondrial transport was assessed in mature iPSC-derived MNs. (A) Representative fluorescent micrograph of iPSC-derived MNs loaded with a selective mitochondrial marker (MitoTracker-Red). **(B)** Representative kymographs are shown for both control and patients cell lines. In each kymograph, the *x* axis represents the position along the axon and the *y* axis represents time. Stationary mitochondria appear as

vertical lines and moving mitochondria generate tilted lines (right= anterograde; left = retrograde). Left scale bar: 20 µm. Time (t) scale bar: 50 s. Distance from cell body (d) scale bar: 50 µm.

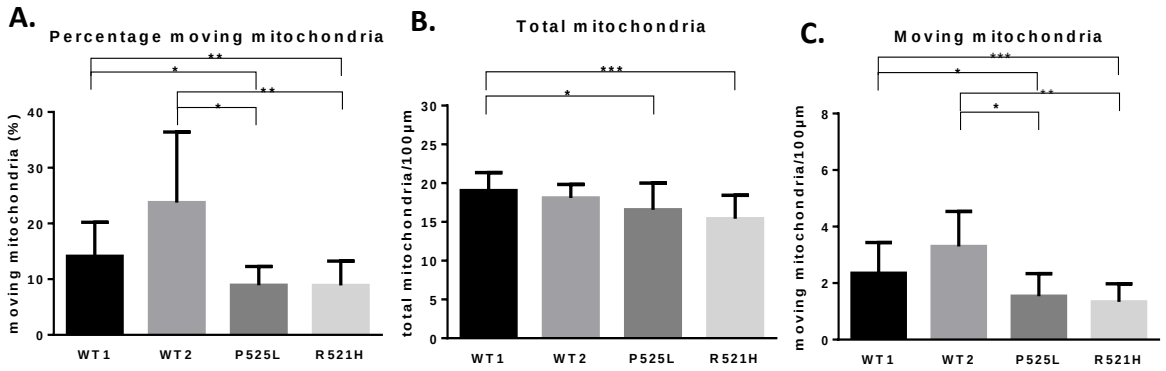

Figure 17. Mitochondrial transport defects of mature iPSC-derived MNs (day 32). Quantification of **(A)** the percentage of moving mitochondria, **(B)** total mitochondria per 100 µm and **(C)** moving mitochondria per 100 µm. Mitochondrial transport was analyzed at day 32 of the differentiation protocol with the use of MytoTracker. Data are represented as mean ± SD. * = $P < 0.05$; ** = $P < 0.01$; *** = $P < 0.005$. Number of measured neurites: WT1 = 15; WT2 = 4; FUS P525L= 22; FUS R521H= 25.

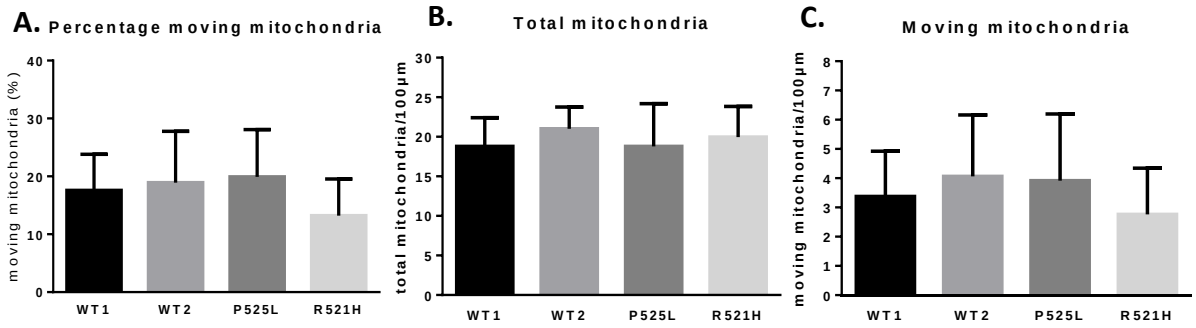

Figure 18. Mitochondrial transport data of mature iPSC-derived MNs (day 35) in the presence of glial cells. Quantification of **(A)** the percentage of moving mitochondria, **(B)** total mitochondria per 100µm and **(C)** moving mitochondria per 100µm. Mitochondrial transport was analyzed with the use of MytoTracker. Data are represented as mean ± SD. * = $P < 0.05$; ** = $P < 0.01$; *** = $P < 0.005$. Number of measured neurites: WT1 = 15; WT2 = 4; FUS P525L= 22; FUS R521H= 25

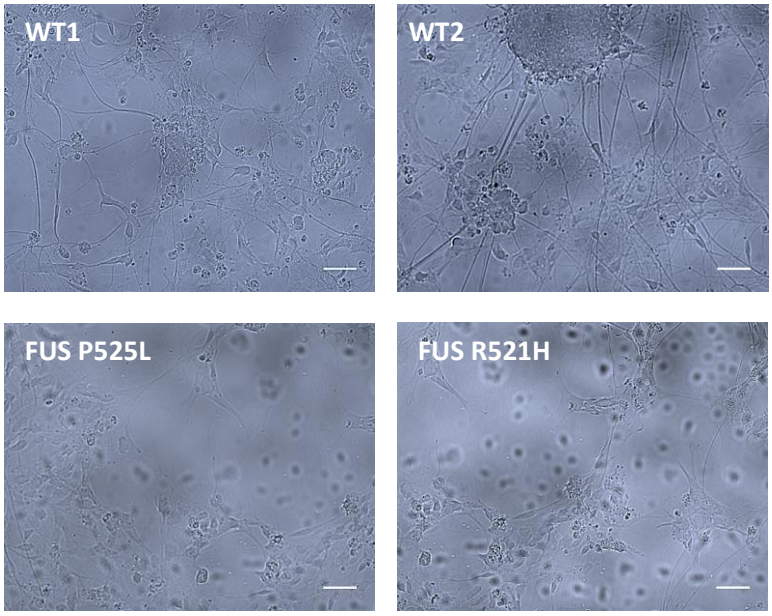

Figure 19. Presence of glial cells, probable astrocytes, in the iPSC-derived MN cultures. Representative bright field images are shown of 32-days-old cultures. Scale bar= 20 µm.

4.2.3 Lysosomal transport defects in a subset of iPSC-derived MNs of ALS patients harbouring a FUS mutation

To investigate whether only mitochondrial transport is disrupted or fast axonal transport in general and because lysosomes are crucial for neuronal functioning, lysosomal transport was analyzed using time lapse imaging approaches in iPSC-derived mature MNs. Lysosomes were stained and tracked with the use of the acid vesicle tracer LysoTracker Red. Fluorescent images were captured over a time period of 200 seconds with a one-second interval. The movies were then converted into kymographs to quantify total and moving lysosomes (Fig. 20-Fig. 23B). The longest distance away from the cell body that a LysoTracker-stained vesicle could be detected was also calculated. Significant differences between patient and control cell lines were detected for this last parameter (Fig.21A WT1= 109.1 $\pm$ 31.8 µm; WT2= 135.1 $\pm$ 32.1 µm; FUS P525L= 68.4 $\pm$ 58.8 µm; FUS R521H= 73.7 $\pm$ 70.0 µm). In iPSC-derived MNs harbouring a FUS mutation this distance was reduced, suggesting that lysosomal transport deficits are indeed present. It should be noted that a high variability in this parameter was present in patient cell lines, which can explain why there is no significant difference between the WT1 and FUS R521H cell line. In order to have a closer look at the obtained results, data of the patient cell lines were subdivided into two groups: one group with data falling in the ”normal range group”, defined as above the lower 95% confidence interval (CI) of control cell lines, and a second group with data falling below this lower 95% CI (Fig. 21). 64% (9 out of 14) (vs. WT1) and 71% (10 out of 14)(vs. WT2) of the measured neurites of both FUS P525L and FUS R521H were falling out the “normal range group”, indicating that an important subset of neurons

harbouring a FUS mutation have disturbed lysosomal transport (Fig. 21A). In addition, a lower number of lysosomes per 100 µm was observed in patient cell lines (Fig. 21B; number per 100 µm: WT1= 6.8 ± 3.1; WT2= 8.0 ± 2.9; FUS P525L= 4.9 ± 3.5; FUS R521H= 4.9 ± 4.1). This difference was only significant when compared to WT2 MNs. It should be stressed that possible accumulation of lysosomes at the beginning of the neurite, due to transport deficits, can disturb the interpretation of this parameter when interpreted alone. No significant differences in the percentage of moving lysosomes were observed (Fig. 21C WT1= 36.55 ± 24.70%; WT2= 43.42 ± 24.70%; FUS P525L= 59.23 ± 36.04%; FUS R521H= 58.41 ± 36.51%), although there is a trend to an increased percentage of movement in patient cell lines. But, patient cell lines showed a lower percentage of retrogradely moving lysosomes in comparison to control cell lines (Fig.23A-B WT1= 80 ± 30%; WT2= 82 ± 31%; FUS P525L= 61 ± 39%, FUS R521H= 45 ± 46% with n=12; 14; 12; 10 respectively). This is a clear but not significant difference, what is most likely due to the very high variability in patient cell lines. This high variability can be explained by the observation that observed transport defects were only present in a subset of FUS-mutated neurons. These results suggest that lysosomal deficits might occur in FUS-ALS MNs.

These differences were not observed in a second differentiation batch (Fig. 22). This was the same differentiation batch as the one used for mitochondrial transport measurements shown in figure 18, in which the presence of glial cells was noticed (Fig. 19).

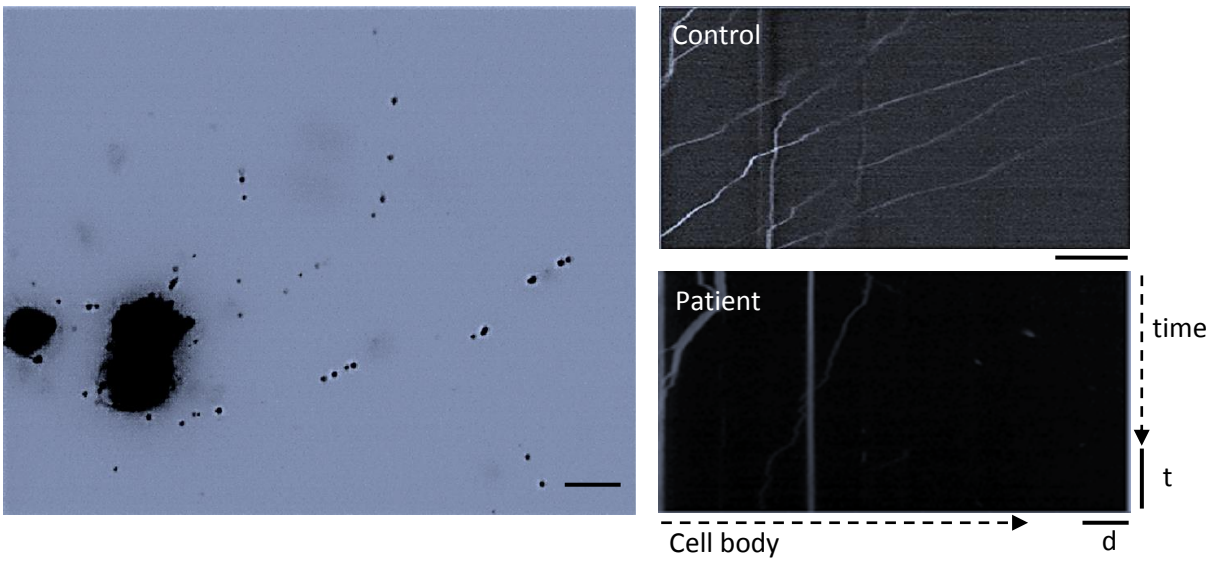

Figure 20. Lysosomal transport was assessed in mature iPSC-derived MNs. (A) Representative fluorescent micrograph of iPSC-derived MN loaded with LysoTracker RED are shown. **(B)** Representative kymographs are shown for both control and patients cell lines. In each kymograph, the *x* axis represents the position along the neurite and the *y* axis represents time. Stationary lysosomes appear as vertical lines and moving lysosomes generate tilted lines (right= anterograde; left = retrograde). Left scale bar: 20 µm. Time (t) scale bar: 50 s. Distance from cell body (d) scale bar: 10 µm.

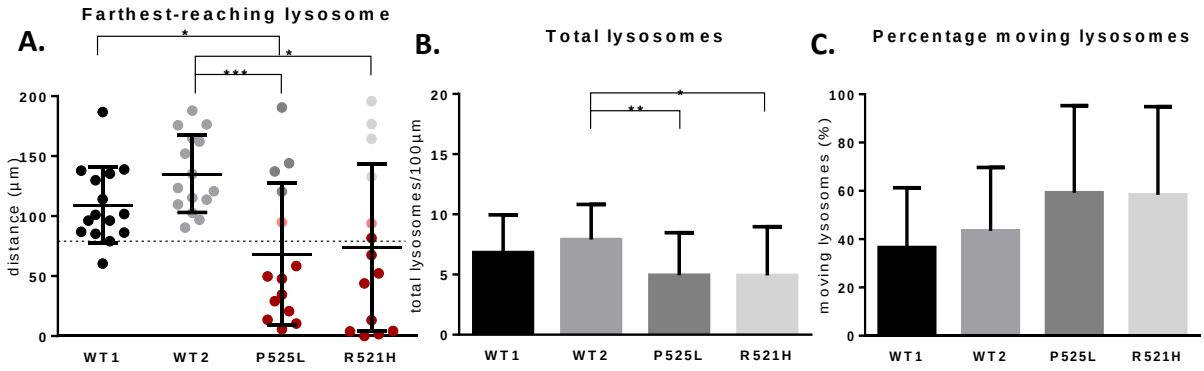

Figure 21. Lysosomal transport defects of mature iPSC-derived MNs (day 32). Quantification of **(A)** the longest distance from the cell body that a LysoTracker-stained lysosome could be detected, **(B)** total lysosomes per 100 µm and **(C)** percentage of moving lysosomes are shown. Lysosomal transport was analyzed at day 32 of the differentiation protocol with the use of a LysoTracker RED staining. **(A)** Dark red dotes= data lying below the lower 95% CI of WT1 (91.4 µm). Light and dark red dotes= data lying below the lower 95% CI of WT2 (117.4 µm). Patient data can be subdivided into two groups: grey spots= data within the "normal range group" and red spots= data without the "normal range group". Dotted line= 80 µm = minimal measured neurite length. Data are represented as mean ± SD. * = $P < 0.05$; ** = $P < 0.01$; *** = $P < 0.005$. Number of measured neurites: WT1 = 15; WT2 = 15; FUS P525L= 14; FUS R521H= 14.

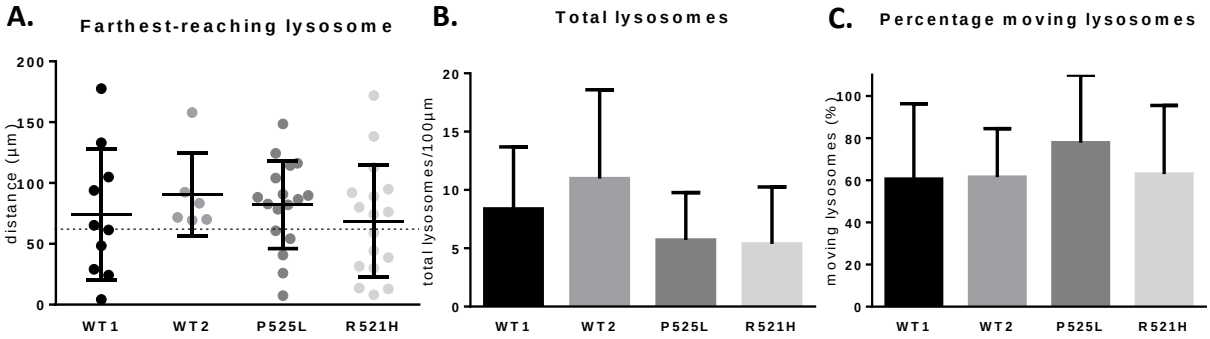

Figure 22. Lysosomal transport data of mature iPSC-derived MNs in the presence of glial cells (day 32) Quantification of **(A)** the longest distance from the cell body that a LysoTracker-stained lysosome could be detected, **(B)** total lysosomes per 100 µm and **(C)** percentage of moving lysosomes are shown. Lysosomal transport was analyzed at day 32 of the differentiation protocol with the use of a LysoTracker RED staining. **(A)** Dotted line= 60 µm = minimal measured neurite length. Data are represented as mean ± SD. * = $P < 0.05$; ** = $P < 0.01$; *** = $P < 0.005$. Number of measured neurites: WT1 = 13; WT2 = 7; FUS P525L= 17; FUS R521H= 19.

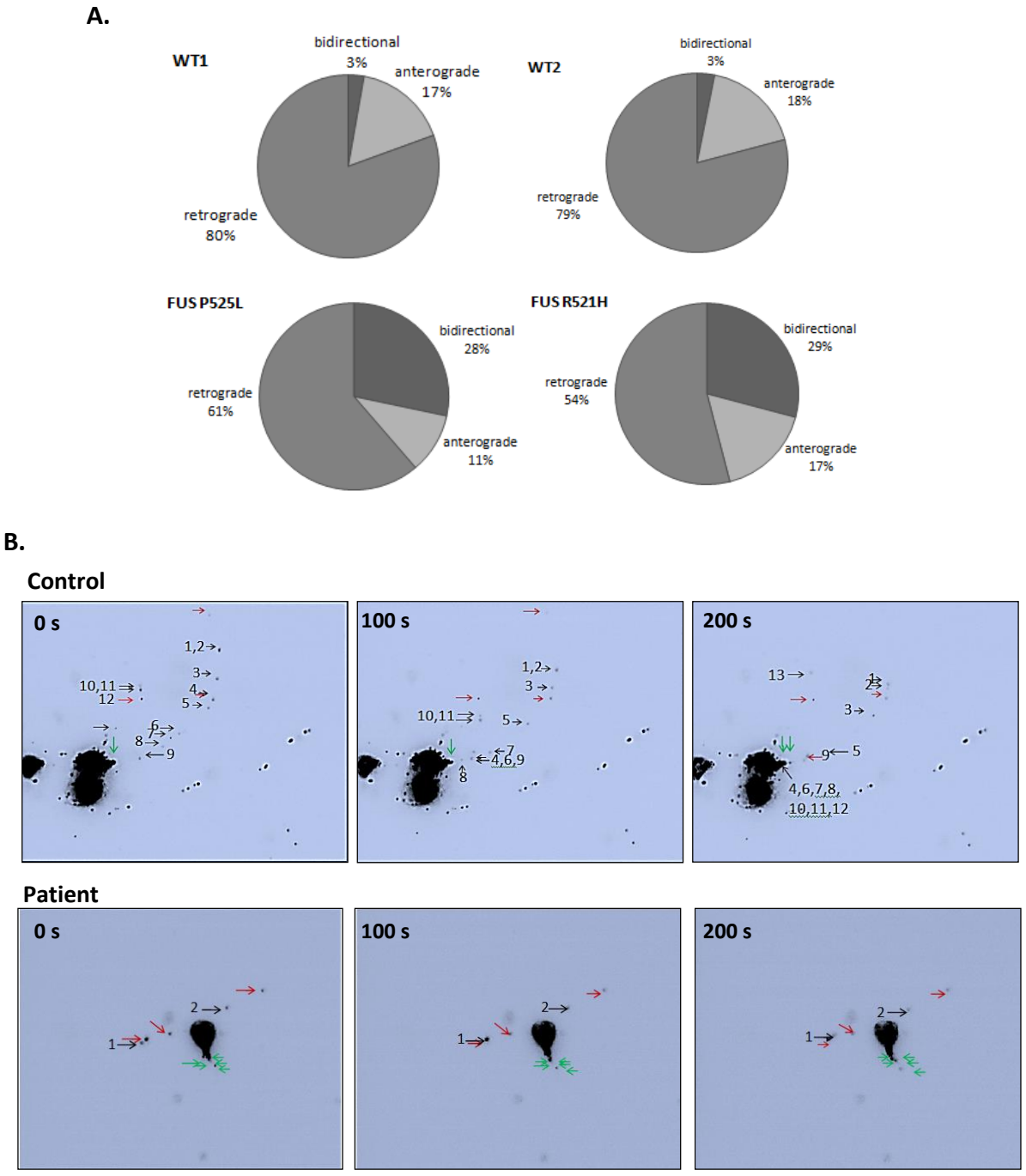

Figure 23. A decrease in the percentage of retrograde moving LysoTracker-positive vesicles in patient cell lines. (A) Mean percentage of bidirectional, anterograde and retrograde moving LysoTracker-positive vesicles per neurite. Measured neuritis: WT1= 12; WT2: 14; FUS P525L= 12; FUS R521H= 10. **(B)** Representative bright field images of LysoTracker based transport analysis are shown. Black arrow= retrogradely moving vesicle; red arrow= stationair vesicle; green vesicle= bidirectionally moving vesicle.

Chapter 5: Discussion and conclusion

ALS is a complex disease in which multiple pathogenic mechanisms are suggested to be involved (10). The lack of understanding of the temporal involvement of each of these pathological factors is a major obstacle in the development of effective therapies for ALS. In this thesis, disturbances in mitochondrial transport and lysosomal deficits were observed in iPSC-derived MNs of ALS patients harbouring a mutation (R521H or P525L) in the NLS of the FUS protein. These deficits occurred in the absence of cell death, which suggests an impairment of axonal transport as an early pathological mechanism in FUS-associated ALS or the necessity of additional stress factors to induce neurodegeneration. This thesis also demonstrates the potential of human MNs derived from iPSCs as a model to study ALS.

5.1 iPSC-derived motor neuron characterization: both control and patient iPSCs differentiate with high efficacy into motor neurons

ALS is a dramatic neurodegenerative disorder characterized by selective UMN and LMN degeneration. This unexplained MN wasting results in paralysis and death of the patient due to respiratory failure within 2 to 5 years after symptom onset. Apart from riluzole, which is a moderately performing drug, no treatment is available. A major barrier to new drug development is the paucity of good models. One solution is to differentiate MNs of iPSCs derived from ALS patients. In this thesis, iPSCs derived from two ALS patients harbouring a mutation in the NLS of FUS and two healthy controls were differentiated into MNs. The used iPSC lines expressed pluripotency markers and in both patient cell lines the original FUS mutation was maintained.

To get insights into the equivalency of *in vitro* derived MNs to bona fide cells at least 4 characteristics need to be assessed (101). First, a multipolar neuronal morphology and the expression of at least a subset of MN markers is a minimal requirement (119). In this thesis, neurons exhibiting typical **MN morphology** were observed. Additionally, MNs can be distinguished from other neurons based on the expression of **MN markers** (119). While no single marker is MN specific, the co-expression of two or three markers can provide reliable criteria for MN identification (103). In this thesis, iPSC-derived neurons expressing the MN transcription factors Hb9 and Isl1 were observed. The vast majority (>70%) of the differentiated cells were positive for Isl1 at the end of the differentiation process, indicating a relatively high differentiation efficacy that is one of the highest in comparison with other published differentiation protocols (120–124). However, it was shown that Isl1 (and Hb9) are each expressed in only a subset of MNs (120). This could lead to an underestimation of the number of MNs when only based on Isl1-staining. On the other hand, Isl1 and Hb9 are also expressed in non-

MNs. For example, Isl1 is also involved in the development of sensory neurons (125). This indicates that awareness is needed when using the number of Isl1-positive neurons as an indication of total MNs (120). In addition, Hb9 can be expressed in a subset of spinal interneurons (126). Hb9 is rapidly down regulated in a subset of brachial and lumbar limb-innervating LMNs (103). This can explain why day 32 iPSC-derived MNs were Hb9-negative. As a consequence, the MN markers Smi32, which is an antibody that recognizes LMN-enriched neurofilament heavy chain, and Chat, which is a marker for cholinergic neurons, can be used to characterize more mature MNs. Smi32 and Chat positive neurons were observed on both day 17 (end of MN differentiation protocol) and day 32 (mature MNs) of the differentiation protocol. Remarkably, the expression of these mature MN markers was already observed on day 17 of the differentiation protocol, when the MNs are suggested to be immature. This is also in contrast to the original article describing the protocol used, in which the MNs are claimed to be Chat-negative at day 17 (117). The immaturity was further supported in this article by immature spikes in response to a current injection (117). The observed difference could be due to a difference in the affinity of the antibodies used. It could also be an illustration of one of the biggest challenges of iPSC-modelling: the variation among individuals and amongst laboratories due to slight variations in the differentiation conditions. However, expression of Smi32 and Chat at day 17 does not automatically indicate that these MNs are already fully maturated. Based on the morphology of these neurons at day 17 (less branched neurites in comparison to day 32), the expression of the embryonic MN marker Hb9 and the lower expression of Chat in comparison to day 32, suggest that the MNs are still immature at day 17 and are only starting to mature. To confirm this hypothesis, the electrophysiological functionality should be analyzed from day 17 on, what we are currently doing in the lab.

The main function of MNs is to innervate target muscles and transduce signals from the CNS to allow voluntary movements of the body. This implies a second and third characteristic of MNs that should be analyzed, namely the ability to form NMJs on muscle fibers and the ability to transmit electrochemical signals (119). Patch clamp recordings showed indeed that the iPSC-derived MNs of both patient and control cell lines exhibited **electrophysiological characteristics** relevant for MN functioning after maturation (day 32). Additional evidence to proof that the generated neurons are MNs and that they are able to recapitulate there *in vivo*-counterparts is to analyze their ability to form NMJs. This can be done by coculturing them with myotubes. The fourth characteristic and the ultimate evidence would be to perform a transplantation experiment into adult spinal cords (of chicken embryos) and to analyze if they are able project to appropriate targets and form NMJs (119). This was however beyond the scope of this master thesis.

In conclusion, the differentiated neurons expressed the pan-neuronal marker βIII-tubulin, the embryonic MN marker Hb9 and the mature MN markers Isl1, Smi32 and Chat. Additionally, neurons exhibited typical multipolar MN morphology and based on patch clamp recordings they were proven to be electrophysiologically active. No significant differences were observed between patient and control cell lines. As a consequence, it can be concluded that the ALS-causing mutations in FUS do not dramatically influence the differentiation of iPSC into MNs. This is in line with our hypothesis that FUS mutations would not interfere with MN development as ALS does not manifest itself until adulthood and it is also in accordance with previous reports (127,128).

A limitation of the protocol used in this thesis (and mainly in all published articles) is mainly the focus on deriving spinal MNs in general without any further diversification of MN subtypes. This will be essential because not all somatic MNs are affected equally by the events leading to neurodegeneration during ALS (129). For example, fast-twitch fatigable (FF) MNs are more susceptible to the neurodegenerative process then fast-twitch resistant (FR) and slow-twitch fatigue resistant (SR) MNs (129). ALS affects the function of very specific MN subtypes (called vulnerable MNs) whereas closely related neurons such as oculomotor MNs are spared (resistant MNs). Because, most neurodegenerative diseases affect specific populations of neurons, reliably differentiating cells into specific homogeneous subtypes is probably one of the greatest challenges that have to be overcome in iPSC technology. For further specification of individual neuronal subtypes analyzing the temporal and spatial expression pattern of Hox proteins can be used (130). Moreover, the used MN differentiation protocol focused on LMN differentiation and not on UMN differentiation, although both are affected in ALS.

In conclusion, we successfully differentiated healthy control and FUS-ALS patient-specific iPSCs into mature MNs but it should be kept in mind that a population of different MN subtypes is obtained and although there was a high MN differentiation efficacy, the MN differentiation is still not 100% efficient.

5.2 ALS phenotype characterization: FUS-ALS iPSC-derived motor neurons recapitulate disease-specific phenotypes

iPSC technology has the potential to revolutionize our understanding of ALS because it gives us the unique opportunity to investigate molecular mechanisms of disease development in neurons containing a patient-specific genetic background. Moreover, it gives us the opportunity to investigate

sporadic ALS, which accounts for 90% of the ALS cases, and numerous ALS gene mutations for which there are no animal models. However, the question remains how well these cells recapitulate the processes seen in ALS patients.

Interestingly, FUS mutations and pathology seem to be important in early-onset ALS and are associated with an aggressive disease course (84,131–133). One of our iPSC lines was derived from a seventeen-year old ALS patient with the *de novo* mutation P525L in the FUS protein. This mutation is indeed associated and overrepresented in early-onset ALS (40%) (84,131). Moreover, the patient died 15 months after the first symptoms, indicating an aggressive disease progression. The parents were negative for this mutation and the control cell lines WT1 and WT2 were derived from the fibroblasts of the father and mother, respectively. The second ALS patient, of whom an iPSC line was derived, was a 71 year old ALS patient carrying the inherited mutation R521H. This "benign" FUS mutation is, in contrast to the "malign" P525L mutation, associated with late onset ALS (134). Both mutations occur in the NLS of FUS and have been shown to cause cytoplasmic mislocalization of FUS (17,49), which was suggested to be the first hit in the pathophysiological cascade that leads to neurodegeneration (83). **Cytoplasmic mislocalization of mutant FUS (R521H and P525L)** was indeed observed in both fibroblasts and iPSC-derived MNs in this thesis. This is similar to previous reports in which significant cytoplasmic mislocalization of FUS-P525L in iPSC-derived MNs of an ALS patient was shown (127). Patient-derived iPSC-derived MNs expressing endogenous R521H FUS were not reported before. However, cytoplasmic mislocalization of R521H FUS has been show in transfected CV1-cells (17,135) and in transfected rat cortical neurons (17). Moreover, it was found that the degree of cytoplasmic displacement of FUS is correlated with the severity of the clinical presentation and age of onset (49,86,87,115,136). The cell line expressing the young-onset causing mutation P525L showed indeed a stronger FUS cytoplasmic staining in patient-derived fibroblasts, in undifferentiated iPSCs and in iPSC-derived MNs in comparison to the "benign" R521H mutant. Interestingly, there was already an obvious cytoplasmic mislocalization of FUS present in undifferentiated iPSCs of P525L mutant cell lines. This highlights an unresolved key aspect of ALS (and other adult-onset neurodegenerative disorders): although mutant protein is expressed from the beginning of life, neurodegeneration only appears later in life. Cytoplasmic mislocalization of P525L FUS in undifferentiated iPSC lines was also observed in a study using FUS P525L iPSC-derived MNs created by TALEN-directed mutagenesis (115). In the same study, undifferentiated patient-derived iPSCs carrying the mutation R521C (R521H was not used in this study) presented only a minute cytoplasmic mislocalization (115), which is similar to our findings. The observation that a "malign" mutation in FUS causes cytoplasmic mislocalization as early as the iPSC stage but a "benign" mutation only after differentiation, was also observed in another study in which iPSC-derived cortical

neurons expressing the benign mutation R521C or the malign mutation R495QfsX527 were used (114).

Besides cytoplasmic mislocalization of mutant FUS, we observed **defects in mitochondrial and lysosomal transport** in the iPSC-derived mature MNs harbouring a FUS mutation. Mitochondria were labelled using a selective marker for functional mitochondria and dynamics were assessed using time-lapse imaging. A significant reduction in the percentage of moving mitochondria in patient-derived MNs was found. Although mitochondrial dysfunction and defective axonal transport of mitochondria has been suggested as a key mechanism in ALS (46,137), no studies investigating mitochondrial transport in iPSC-differentiated MNs derived from FUS-ALS patients were published so far. However, a study in which a *Drosophila* model ectopically expressed FUS P525L did not show a disruption in mitochondrial transport (138). The same approach as for the mitochondria was applied to analyze lysosomal transport. This revealed lysosomal transport deficits in a subset of FUS-mutated neurons. Despite the fact that in patient cells lysosomes were localised closer to the cell body and despite the reduction in number of total lysosomes per 100 µm, we did not detect a reduction in the percentage of moving lysosomes. As LysoTracker RED labels preferentially acidic organelles, this might indicate that there are no lysosomal transport defects, but rather defects in autophagosome maturation (=acidification). Lysosomes are predominantly localized in the soma (139) and move bidirectional close to the cell body (140). In contrast, autophagosomes that are preferentially formed at the distal end of axons mainly undergo retrograde transport, while gradually acidifying (maturating), likely owing to fusion with lysosomes (139,141–143). As a consequence, the presence of lysosomes moving close to the cell body in combination with a decreased acidification of retrogradely moving autophagosomes could explain the observed decrease in distance that LysoTracker-positive vesicles are found from the cell body and the decrease in total acid vesicles when measured over a length of 100 µm. This hypothesis is supported by the observation that in patient cell lines the percentage of retrogradely moving LysoTracker-positive organelles was lower than in control cell lines. Here, the retrogradely moving vesicles could be mature autophagosome that were formed at the synapse and are moving to the cell body (141). Bidirectionally moving vesicles are suggested to be lysosomes moving in the proximal part of the neurite (141). This hypothesis is also in agreement with a study in which FUS P525L overexpression in *Drosophila* resulted in vesicle transport deficits (138). Moreover, disturbance in the autophagy-lysosomal system have been reported in other neurodegerative diseases such as Alzheimer's disease (139,143,144), Parkinson's disease (143,144) and Huntington's disease (143) as well as in the mutant $SOD1^{G93A}$ mouse model (145). In this SOD1-ALS mouse model lysosomal deficits were observed as an early pathological event and were suggested as the basis of axonal transport deficits and

neurodegeneration (145). Our findings are also in line with the observation that expression of R521H and P525L FUS mutants in neurons can cause axonal defects (146). These authors claimed that the observed axonal defects are caused by mutated FUS through reducing axonal levels of survival motor neuron protein (SMN) (146), the causative factor of spinal muscular atrophy (SMA). This hypothesis was based on the observed colocalization of SMN in cytoplasmic FUS aggregates and a rescue experiment through SMN overexpression (146). An association of FUS with SMN in neuronal cell lines was also reported in another study (147). Moreover, it was suggested that the two proteins are involved in the same pathway and that FUS mislocalization to the cytoplasm can cause partial mislocalization of snRNPs that work downstream of SMN (147). Interestingly, it has also been shown that reduction of SMN deregulates autophagy and causes the accumulation of immature autophagosomes in spinal cord MNs *in vitro* (148). Moreover, abnormal mitochondrial transport has been observed as an early pathological change in SMA patient-iPSC differentiated MNs (149). It needs to be further investigated whether there is indeed a disturbance of autophagosome dynamics, autophagosome maturation and/or lysosomal proteolysis in this FUS ALS-model. Moreover, this hypothesis is based on only one observation and should be confirmed. Also the limited technical abilities of LysoTracker RED due to fast bleaching should be taken into account (150), although this should not have caused differences between patient and control cell lines.

It has been shown that this retrograde transport of autophagosomes is essential for their lysosomal maturation and effective degradation of their cargo (139,151). Disturbance in vesicle transport could therefore cause disturbance in autophagy. In combination with mitochondrial transport (and mitochondrial fusion and fission) is mitophagy essential for maintaining mitochondrial quality control (45). Considering that mitochondria are essential for energy production, Ca^{2+} homeostasis and also play an important role in apoptosis, a disturbance in mitochondrial quality control can have serious consequences for neuronal health. Moreover, owing to their high metabolic activity and long axons, MNs are extra depending on mitochondrial transport. There is a lot of evidence for the involvement of mitochondrial dysfunctions in ALS pathology (41). A logical next step would be to investigate the morphology (electron-microscopy), health (by measuring mitochondrial membrane potential), and density (electron-microscopy) of mitochondria in the MNs derived from iPSCs from mutant FUS patients.

The iPSC-derived MNs harbouring a FUS mutation didn't underwent neurodegeneration despite FUS mislocalization and mitochondrial and lysosomal transport defects. As a consequence, it could be that mitochondrial and lysosomal transport defects are an early pathological mechanism and that longer incubation time is necessary to observe neurodegeneration. This was indeed observed in a study of Chen *et al*. in which mutant SOD1 ALS iPSC-derived MNs exhibited bead-like swellings along

neurites and underwent neurodegeneration when kept in culture for longer time (152). The same was observed in iPSC-derived spinal MNs from SMA patients (149). In this culture model, mitochondrial transport defects were observed followed by neurodegeneration. For example, a decrease in ATP supply to motor proteins due to mitochondrial dysfunction can lead to a general decreased axonal transport of proteins, lipids and other organelles (60). Therefore, it could be that transport of other cargos might better correlate with axonal degeneration (47). This is in line with previous finding that in neurons isolated from SOD1 and TDP-43 ALS mouse models mitochondrial transport was affected first, before the onset of symptoms (153). This is also in agreement with the dying-back pattern seen in ALS patients (55). Maintaining axonal homeostasis of MNs requires active mitochondrial and lysosomal transport and therefore consequences of early axonal transport defects will first occur at the distal end of the axon, before MN loss is visible. To investigate whether this is here the case, iPSC-derived MNs can be cocultured with myotubes to analyze if loss of neuromuscular synapses and axonal retraction occur.

The capability of these MNs to survive despite mitochondrial and lysosomal transport defects might also suggest that the observed axonal transport defects are not severe enough to cause neurodegeneration or that some compensatory mechanism might be present. Additional stress factors such as aging or inflammation could be necessary to trigger neurodegeneration. This hypothesis is in line with the second hit hypothesis related to FUS pathology (see above: FUS pathology). In this hypothesis mislocalization of FUS to the cytoplasm is seen as the first hit in the pathophysiological cascade (83). A second hit, such as formation of stress granules due to cellular stress, is necessary to induce neurodegeneration (83). In this thesis, only cytoplasmic mislocalization of FUS was observed and not the possibly required FUS aggregates. This necessity to form stress granules to induce neurodegeneration is supported by the finding that disturbing the RNA-binding domains of FUS, which are essential for incorporation of mutant FUS into stress granules inhibits neurodegenerative phenotype of mutant FUS *in vivo* (154). To test this hypothesis stress could be applied to the cell cultures or aging could be achieved by applying progerin-induced aging (155).

How cytoplasmic mislocalization of FUS leads to the mitochondrial and lysosomal transport defects is not clear. It is hypothesized that this mislocalization can cause a loss of nuclear function, a toxic cytoplasmic gain-of-function or both. FUS is involved in gene transcription, pre-mRNA splicing and mRNA transport. This raises the possibility that impaired axonal transport might be a direct consequence of the loss of the nuclear function of FUS in translation and RNA biogenesis. For example, it has been shown that FUS binds and regulates RNAs of several motor proteins such as KIF5C, KIF1B and KIF3A (156,157). These three kinesin motor proteins are involved in axonal

transport of both mitochondria and vesicles. Moreover, increased interaction with cytoplasmic RNA targets that are involved in axonal transport, and which might disrupt their function, might play a role. To confirm whether the observed abnormal mitochondrial dynamics and lysosomal deficits are directly linked to mutant FUS, analyzing axonal transport after genetically correcting the FUS mutation is essential. In addition, considering that MNs specifically degenerate in ALS patients, investigating whether the observed defects are specific to iPSC-derived MNs or not would be an interesting study.

We observed that in one of the differentiation batches no differences in both mitochondrial and lysosomal transport were observed between any of the four cell lines. The only observed difference between this differentiation batch and the others was the presence of a large number of cells that could be astrocytes. It is not clear what the reason could be for this. It could be that these cells have a protective effect on MN functioning. This hypothesis is however in contrast with the general accepted hypothesis that astrocytes have an active role in MN death in ALS (158). However, ALS is a clinically heterogeneous disease and most studies supporting this hypothesis have made use of mutant SOD1 ALS models (158) and thus don't proof that astrocyte-mediated MN toxicity is a universal phenomenon of ALS. This statement is supported by the observation that astrocytes with TDP-43 alterations did not adopt a toxic phenotype and did not cause death of WT MNs in culture (159). The same observation was made in a study that used iPSC-derived astrocytes obtained from ALS patients with a TDP-43 mutation in co-culture with WT MNs (160). Moreover, it was shown that co-culturing alsin-depleted spinal MNs with astrocytes rescues them from defective survival and axon growth (161). Recessive mutations in Alsin have been reported in juvenile forms of ALS (162). Based on the functional and structural similarities between FUS and TDP-43 (in contrast to SOD1) the same might be true for FUS-associated ALS.

In conclusion, this study demonstrated the potential of human MNs-derived from iPSCs as a model for studying ALS. Mutant FUS mislocalization to the cytoplasm, which also occurs in pathological conditions, was observed. In addition, mitochondrial transport and lysosomal deficits were detected. However, whether and how FUS cytoplasmic mislocalization results in the transport deficits needs to be further elucidated.

Chapter 6: Dutch Summary

6.1 Amyotrofe laterale sclerose

Amyotrofe laterale sclerose (ALS) is een neurodegeneratieve ziekte waarbij de patiënt progressief krachtsverlies ondervindt en geleidelijk aan verlamd wordt. De onderliggende oorzaak is het **afsterven van de motorische neuronen** (MNn) in de motorische hersenschors, de hersenstam en het ruggenmerg (2). De patiënt sterft uiteindelijk door verlamming van de ademhalingsspieren en dit ongeveer 2 tot 5 jaar na diagnose (3). Tot op vandaag is het onderliggende mechanisme van dit verlies aan MNn ongekend. De huidige hypothese is dat ALS wordt veroorzaakt door een combinatie van verschillende pathologische processen (32) zoals excitotoxiciteit, oxidatieve stress, mitochondriale dysfunctie, verstoring van het axonaal transport, endoplasmatische reticulum stress, neuroinflammatie en abnormale RNA verwerking (10). Hoewel sommige van deze pathologische mechanismen individueel goed gekend zijn, blijft hun onderlinge verband en bijdrage onduidelijk.

De eerste symptomen doen zich bij de meeste patiënten voor op volwassen leeftijd, met een gemiddelde van 55 jaar oud (11). Een westerse vrouw heeft een risico van 1 op 472 om gedurende haar leven ALS te ontwikkelen, een man 1 op 350 (9). Hiermee is ALS de meest voorkomende vorm van volwassen motorneuronziekte. ALS komt voornamelijk sporadisch voor (sporadische ALS, sALS), maar in 10% van de gevallen is er een familiaal voorkomen (familiale ALS, fALS) (6). In de meerderheid van de ALS-patiënten waarbij er sprake is van fALS is de genetische oorzaak gekend. De belangrijkste geïdentificeerde ALS genen zijn: *superoxide dismutase 1* (*SOD1*), *fused in sarcoma* (*FUS*), *TAR-DNA binding protein* (*TARDBP*) en chromosome 9 open reading frame72 (*C9ORF72)* (7).

Mutaties in **FUS** zijn verantwoordelijke voor 4% van de fALS en 1% van de sALS gevallen (6). Opmerkelijk is dat mutaties in FUS de belangrijkste oorzaak zijn van vroegtijdige ALS en vaak met een snel progressief verloop geassocieerd zijn (84,131). FUS is een DNA/RNA bindend eiwit dat tussenkomt in meerdere cellulaire functies, zoals gen transcriptie, translatie en mRNA transport (83). FUS bevindt zich voornamelijk in de nucleus, maar kan zich verplaatsen van de nucleus naar het cytoplasma en omgekeerd door de aanwezigheid van een nucleair export signaal (NES) en een nucleair lokalisatie signaal (NLS) (49). Het NLS is aanwezig in het C-terminaal gedeelte van FUS, waar het merendeel van de ALS-geassocieërde mutaties voorkomen (26). Deze mutaties verstoren het NLS en zorgen hierdoor voor een mislokalisatie van FUS naar het cytoplasma (49). Deze cytoplasmatische mislokalisatie kan zorgen voor het verlies van de functies van FUS in de nucleus en/of het verkrijgen van toxische eigenschappen in het cytoplasma. Daarom wordt gesuggereerd dat mislokalisatie van FUS naar het cytoplasma een belangrijke rol speelt in de pathologische cascade van FUS-

geassocieerde ALS. Hoe mislokalisatie van FUS naar het cytoplasma neurondegeneratie veroorzaakt is voorlopig niet geweten.

Op dit moment is slechts één matig werkend medicijn geregistreerd voor de behandeling van ALS, met name Riluzole (12). Dit heeft als gevolg dat de behandeling voornamelijk uit ondersteunende therapieën bestaat. Een belangrijk hindernis bij de ontwikkeling van nieuwe geneesmiddelen is het ontbreken van goede modellen. Geïnduceerde pluripotente stamcellen (iPS cellen) geven ons de mogelijkheid om deze hindernis te overwinnen (13). Vanuit de huidcellen van ALS patiënten kunnen iPS cellijnen worden verkregen (100). Deze cellen kunnen vervolgens in MNn worden gedifferentieerd met dezelfde genetische achtergrond als de individuele ALS patiënten. Een belangrijke vraag blijft natuurlijk in welke mate de MNn die op deze manier verkregen worden gelijk zijn aan hun *in vivo* tegenhangers en in welke mate de ALS pathologie aanwezig is.

6.2 Doelstellingen

De eerste doelstelling in deze thesis is om iPS cellen, afkomstig van ALS-patiënten met aan mutatie in FUS en gezonde controles, in motorische neuronen te differentiëren. Vervolgens werd nagegaan of een ALS fenotype aanwezig is in de MNn afkomstig van de ALS patiënten (Fig. 1).

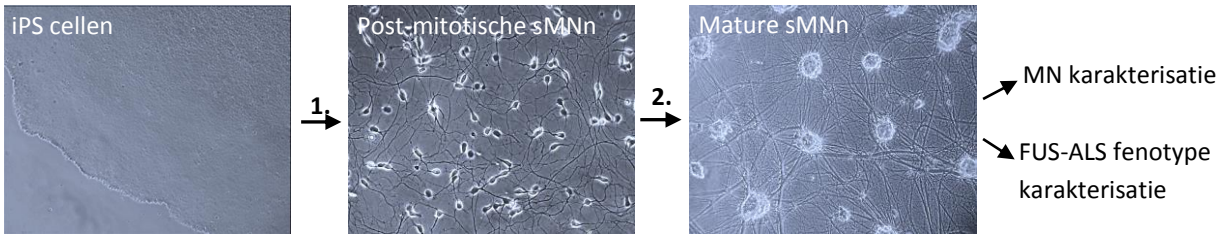

Figuur 1. Differentiatie van iPS cellijnen in spinale motorische neuronen. **(1) MN differentiatie**. iPS cellen werden eerst gedifferentieerd in immature MNn. Een representatieve foto van een 17-dagen oude cultuur is weergegeven. **(2) Maturatie**. Vervolgens werden de cellen nog in cultuur gehouden voor verder ontwikkeling tot dag 32. Een representatie foto van 32-oude cultuur is weergegeven. iPS cellen= geïnduceerde pluripotente stamcellen. sMN= spinale motorische neuronen.

6.3 Methoden, resultaten en discussie

6.3.1. Differentiatie in motorische neuron en karakterisatie

Om de onderliggende pathologische mechanismen van gemuteerd FUS in ALS te onderzoeken, werden in deze thesis iPS cellijnen gebruikt afkomstig van twee FUS-ALS patiënten en twee gezonde personen. De eerste ALS patiënt was een 71-jarige vrouw die drager is van de R521H mutatie in de NLS of FUS. De tweede ALS patiënt was een 17-jarige jongen waarbij de P525L mutatie in de NLS of van FUS werd vastgesteld. De ouders waren negatief voor deze mutatie. iPS cellijnen afkomstig van

de vader en moeder van deze ALS patiënt werden dan ook als controles gebruikt. De iPS cellijnen van zowel ALS patiënten als controles werden in parallel gedifferentieerd in spinale MNn, volgens het differentiatie protocol van Maury *et al*. (117). Eerst werd een neuronale identiteit geïnduceerd door inhibitie van BMP-signalering (LDN en SB) en stimulatie van Wnt-signalering (CHIR). Vervolgens werd caudalizatie geïnduceerd (retinoic acid, RA), gevolgd door inductie van een MN-identiteit (ventralizatie) (smoothened agonist, SAG en RA). MN-diffentiatie nam 17 dagen in beslag. Vervolgens werden de cellen nog in cultuur gehouden voor verdere ontwikkeling tot dag 32 (Fig. 1). Op basis van immunologische kleuringen werden de gedifferentieerde cellen positief bevonden voor verschillende **MN-merkers**. Hoewel geen enkele merker op zichzelf MN-specifiek is, is de expressie van een combinatie van 2 tot 3 betrouwbaar voor MN identificatie (103). Na MN-differentiatie (dag 17) brachten de gedifferentieerde neuronen de pan-neuronale marker βIII-tubuline, de embryonale MNn merker Hb9 en de mature MNn merkers Isl1, Smi32 en Chat tot expressie. De meerderheid van de gedifferentieerde neuronen waren Isl1-positief (>70%). Dit suggereert een hoge differentiatie van iPS cellen in MNn. Na verdere ontwikkeling (dag 32), werd βIII-tubuline en de mature MNn markers Isl, Smi32 en Chat nog steeds tot expressie gebracht. De embryonal MN-merker Hb9 was afwezig. Naast de expressie van MN-merkers werd ook een typische **MN-morfologie** waargenomen: een multipolair neuron met een lang axon. Bovendien werd met behulp van patch-clamp metingen aangetoond dat de MNn op dag 32 **spontaan actiepotentialen** vuurden die karakteristiek zijn voor mature en functionele MNn.

We concluderen dat we zowel de cellijnen afkomstig van gezonde controles als ook van ALS patiënten met een hoge efficiëntie konden differentiëren in functionele en mature MNn. Dit wijst erop dat de P525L en R521H mutaties in FUS geen grote invloed hebben op de differentie van iPS cellen in MNn. Dit is in overeenkomst met het feit dat ALS zich pas op volwassen leeftijd manifesteert.

6.3.2 FUS-ALS fenotype karakterisatie

In het twee deel van deze thesis werd onderzocht of in de gedifferentieerde MNn ook een FUS-ALS fenotype aanwezig was. Beide ALS iPS cellijnen zijn afkomstig van ALS patiënten met een mutatie in de NLS van FUS. Er wordt verondersteld dat dit soort mutaties pathologisch is omdat ze een mislokalisatie van FUS naar het cytoplasma veroorzaken (49). Daarom werd met behulp van een immunologische kleuring de cellulaire lokalisatie van FUS nagegaan. In fibroblasten afkomstig van beide ALS patiënten werd cytoplasmatische mislokalisatie van FUS waargenomen. Een duidelijke mislokalisatie van FUS naar het cytoplasma was ook zichtbaar in de ongedifferentieerde iPS cellijnen die P525L FUS tot expressie brengen. **Mislokalisatie van gemuteerd FUS** was ook waarneembaar in

de gedifferentieerde MNn (dag 17 en dag 32) afkomstig van beide patiënt cellijnen. Deze bevindingen komen overeen met wat reeds gepubliceerd werd (17,127,135). Bovendien werd een sterkere cytoplasmatische kleuring geobserveerd in fibroblasten, in ongedifferentieerde en in gedifferentieerde iPS cellen die P525L FUS tot expressie brachten in vergelijking met R521H FUS. Dit is in overeenkomst met de hypothese dat een sterkere FUS mislokalisatie gerelateerd is aan een vroegere leeftijd waarop ALS zich manifesteert en een sneller ziekte verloop (49,86,87,115,136).

Er wordt gesuggereerd dat een verstoord mitochondriaal transport een rol speelt in de eerste fasen van de pathogenese van ALS. Daarom werd met behulp van een mitochondriale kleuring (MitoTracker-RED) en "time-lapse imaging" mitochondriaal transport onderzocht in iPS cel-afgeleide mature MNn (dag 32). Gedurende 200 seconden werd met een één-seconde interval foto's genomen en deze video's werden vervolgens in "kymographs" omgezet om de mobiliteit van de mitochondriën te analyseren. Een significante **afname in het percentage bewegende mitochondriën** in patiënt-MNn in vergelijken met controle-MNn werd vastgesteld. Dezelfde strategie werd toegepast voor het analyseren van het lysosomaal transport (LysoTracker-RED kleuring). In een groep van MNn afgeleid van patiënt-iPS cellen werd een **verstoord transport van zure vesikels** vastgesteld. Omdat zowel lysosomen als mature autophagosomen worden gekleurd door LysoTracker, kan dit wijzen op een verstoorde maturatie van autophagosomen. Deze hypothese vereist verder onderzoek, maar een verstoord autophagosoom-lysosomaal systeem kan leiden tot een afgenomen autofagie van mitochondriën (mitofagie). In combinatie met een verstoord mitochondriaal transport heeft dit mitochondriale disfuncties tot gevolg. Hoe de mislokalisatie van FUS de geobserveerde defecten zou kunnen veroorzaken is niet volledig duidelijk. Een verstoorde FUS-geassocieerde transcriptie en translatie kunnen eventueel een rol spelen.

Samengevat tonen we in deze thesis aan dat iPS cellen afkomstig van ALS patiënten met mutaties in de NLS van FUS succesvol kunnen worden gedifferentieerd in MNn. Bovendien werd naast de mislokalisatie van gemuteerd FUS naar het cytoplasma ook een verstoord mitochondriaal transport en mogelijkerwijze ook een verstoorde autophagosoom-lysosomale werking waargenomen. Deze bevindingen tonen aan dat iPS cellen-afgeleide MNn de mogelijkheid bieden om als een humaan model voor ALS gebruikt te worden en dat een verstoord axonaal transport een mogelijke rol kan spelen bij mutant FUS-geassocieerde ALS.

References

1. Robberecht W, Philips T. The changing scene of amyotrophic lateral sclerosis. Nat Rev Neurosci. Nature Publishing Group; 2013;14(4):248–64.

2. Wijesekera LC, Leigh PN. Amyotrophic lateral sclerosis. Orphanet J Rare Dis. 2009;4:3.

3. Rowland LP, Shneider NA. Amyotrophic Lateral Sclerosis. new Engl J. 2001;344(22):1688–700.

4. Iguchi Y, Katsuno M, Ikenaka K, Ishigaki S, Sobue G. Amyotrophic lateral sclerosis: An update on recent genetic insights. J Neurol. 2013;260(11):2917–27.

5. Laferriere F, Polymenidou M. Advances and challenges in understanding the multifaceted pathogenesis of amyotrophic lateral sclerosis. Swiss Med Wkly. 2015;(January):1–13.

6. Renton AE, Chiò A, Traynor BJ. State of play in amyotrophic lateral sclerosis genetics. Nat Neurosci. Nature Publishing Group; 2014;17(1):17–23.

7. Gros-Louis F, Gaspar C, Rouleau G a. Genetics of familial and sporadic amyotrophic lateral sclerosis. Biochim Biophys Acta. 2006;1762(11-12):956–72.

8. Al-Chalabi A, Hardiman O. The epidemiology of ALS: a conspiracy of genes, environment and time. Nat Rev Neurol. Nature Publishing Group; 2013;9(11):617–28.

9. Alonso a., Logroscino G, Jick SS, Hernán M a. Incidence and lifetime risk of motor neuron disease in the United Kingdom: a population-based study. Eur J Neurol. 2009;16(6):745–51.

10. Mancuso R, Navarro X. Amyotrophic lateral sclerosis: Current perspectives from basic research to the clinic. Prog Neurobiol. Elsevier Ltd; 2015 Aug 5;26.

11. Pasinelli P, Brown RH. Molecular biology of amyotrophic lateral sclerosis: insights from genetics. Nat Rev Neurosci. 2006;7(9):710–23.

12. Bensimon G, Lacomblez L, Meninger V, Group AS. A controlled trial of riluzole in amyotrophic lateral sclerosis. N Engl J Med. 1994;330(9):585–91.

13. Richard J-P, Maragakis NJ. Induced pluripotent stem cells from ALS patients for disease modeling. Brain Res. Elsevier; 2014;1607:15–25.

14. Rosen DR, Siddique T, Patterson D, Figlewicz DA, Sapp P, Hentati A, et al. Mutations in Cu/Zn superoxide dismutase gene are associated with familial amyotrophic lateral sclerosis. Nature. 1993;363:210–1.

15. Ajroud-Driss S, Siddique T. Sporadic and hereditary amyotrophic lateral sclerosis (ALS). Biochim Biophys Acta - Mol Basis Dis. Elsevier B.V.; 2015;1852(4):679–84.

16. Mackenzie IR a., Bigio EH, Ince PG, Geser F, Neumann M, Cairns NJ, et al. Pathological TDP-43 distinguishes sporadic amyotrophic lateral sclerosis from amyotrophic lateral sclerosis withSOD1 mutations. Ann Neurol. 2007;61(5):427–34.

17. Vance C, Rogelj B, Hortobagyi T, De Vos KJ, Nishimura AL, Sreedharan J, et al. Mutations in FUS, an RNA processing protein, cause familial amyotrophic lateral sclerosis type 6. 2009;323(February):1208–11.

18. Buratti E, Baralle F. Multiple Roles of TDP-43 in gene expression, splicing regulation and human disease. Front Biosci. 2008;13:867–78.

19. Lagier-Tourenne C, Cleveland DW. Rethinking ALS: the FUS about TDP-43. Cell. 2009;136(6):1001–4.

20. Yang S, Warraich ST, Nicholson G a., Blair IP. Fused in sarcoma/translocated in liposarcoma: A multifunctional DNA/RNA binding protein. Int J Biochem Cell Biol. Elsevier Ltd; 2010;42(9):1408–11.

21. Lissouba A, Liao M, Brustein E, Guy A, Kabashi E. FUS and TARDBP but Not SOD1 Interact in Genetic Models of Amyotrophic Lateral Sclerosis. 2011;7(8):17–28.

22. Baloh RH. How do the RNA-binding proteins TDP-43 and FUS relate to amyotrophic lateral sclerosis and frontotemporal degeneration, and to each other? Curr Opin Neurol. 2012;25(6):1.

23. Lagier-Tourenne C, Polymenidou M, Hutt KR, Vu AQ, Baughn M, Huelga SC, et al. Divergent roles of ALS-linked proteins FUS/TLS and TDP-43 intersect in processing long pre-mRNAs. Nat Neurosci. Nature Publishing Group; 2012;15(11):1488–97.

24. Szafranski K. Non-coding RNA in neural function, disease, and aging. Front Genet. 2015;6(March):1–16.

25. King OD, Gitler AD, Shorter J. The tip of the iceberg: RNA-binding proteins with prion-like domains in neurodegenerative disease. Brain Res. Elsevier B.V.; 2012;1462:61–80.

26. Deng H, Gao K, Jankovic J. The role of FUS gene variants in neurodegenerative diseases. Nat Rev Neurol. Nature Publishing Group; 2014;10(6):337–48.

27. Rademakers R. C9orf72 repeat expansions in patients with ALS and FTD. Lancet Neurol. Elsevier Ltd; 2012;11(4):297–8.

28. Levine TP, Daniels RD, Gatta a. T, Wong LH, Hayes MJ. The product of C9orf72, a gene strongly implicated in neurodegeneration, is structurally related to DENN Rab-GEFs. Bioinformatics. 2013;29(4):499–503.

29. Fratta P, Mizielinska S, Nicoll AJ, Zloh M, Fisher EMC, Parkinson G, et al. C9orf72 hexanucleotide repeat associated with amyotrophic lateral sclerosis and frontotemporal dementia forms RNA G-quadruplexes. Sci Rep. 2012;2:1–6.

30. Lee Y-B, Chen H-J, Peres JN, Gomez-Deza J, Attig J, Štalekar M, et al. Hexanucleotide Repeats in ALS/FTD Form Length-Dependent RNA Foci, Sequester RNA Binding Proteins, and Are Neurotoxic. Cell Rep. 2013;5(5):1178–86.

31. Ling SC, Polymenidou M, Cleveland DW. Converging mechanisms in als and FTD: Disrupted RNA and protein homeostasis. Neuron. Elsevier Inc.; 2013;79(3):416–38.

32. Cozzolino M, Ferri A, Carrì MT. Amyotrophic lateral sclerosis: from current developments in the laboratory to clinical implications. Antioxid Redox Signal. 2008;10(3):405–43.

33. Perry TL, Krieger C, Hansen S, Eisen A. Amyotrophic lateral sclerosis: amino acid levels in plasma and cerebrospinal fluid. Ann Neurol. 1990;28(1):12–7.

34. Van Den Bosch L, Van Damme P, Bogaert E, Robberecht W. The role of excitotoxicity in the pathogenesis of amyotrophic lateral sclerosis. Biochim Biophys Acta - Mol Basis Dis. 2006;1762(11-12):1068–82.

35. Doble A. The Role of Excitotoxicity in Neurodegenerative Disease: implications for therapy. Pharmacol Ther. 1999;81(3):163–221.

36. Arundine M, Tymianski M. Molecular mechanisms of calcium-dependent neurodegeneration in excitotoxicity. Cell Calcium. 2003;34(4-5):325–37.

37. Bellingham MC. A Review of the Neural Mechanisms of Action and Clinical Efficiency of Riluzole in Treating Amyotrophic Lateral Sclerosis: What have we Learned in the Last Decade? CNS Neurosci Ther. 2011;17(1):4–31.

38. Mitsumoto H, Santella R., Liu X, Bodganov M, Zipprich J, Wu H-C, et al. Oxidative Stress Biomarkers in Sporadic ALS. Amyotroph lateral Scler. 2008;9:177–83.

39. Nicholls DG, Budd SL. Mitochondria and Neuronal Survival. Physiol Rev. 2000;80(1):315–60.

40. Wallace DC. A mitochondrial paradigm of metabolic and degenerative diseases, aging and cancer: a dawn for evolutionary medicine. Annu Rev Genet. 2005;39(1):359–407.

41. Cozzolino M, Carrì MT. Mitochondrial dysfunction in ALS. Prog Neurobiol. 2012;97(2):54–66.

42. Sasaki S, Maruyama S, Yamane K, Sakuma H, Takeishi M. Ultrastructure of swollen proximal axons of anterior horn neurons in motor neuron disease. J Neurol Sci. 1990;97(2-3):233–40.

43. Sasaki S, Iwata M. Mitochondrial alterations in the spinal cord of patients with sporadic amyotrophic lateral sclerosis. J Neuropathol Exp Neurol. 2007;66(1):10–6.

44. Kong J, Xu Z. Massive mitochondrial degeneration in motor neurons triggers the onset of amyotrophic lateral sclerosis in mice expressing a mutant SOD1. J Neurosci. 1998;18(9):3241–50.

45. Cai Q, Tammineni P. Alterations in Mitochondrial Quality Control in Alzheimer's Disease. Front Cell Neurosci. 2016;10(February):1–17.

46. Millecamps S, Julien J-P. Axonal transport deficits and neurodegenerative diseases. Nat Rev Neurosci. Nature Publishing Group; 2013;14(3):161–76.

47. Chevalier-Larsen E, Holzbaur ELF. Axonal transport and neurodegenerative disease. Biochim Biophys Acta. 2006;1762(11-12):1094–108.

48. Pasinelli P, Belford ME, Lennon N, Bacskai BJ, Hyman BT, Trotti D, et al. Amyotrophic lateral sclerosis-associated SOD1 mutant proteins bind and aggregate with Bcl-2 in spinal cord mitochondria. Neuron. 2004;43(1):19–30.

49. Dormann D, Rodde R, Edbauer D, Bentmann E, Fischer I, Hruscha A, et al. ALS-associated fused in sarcoma (FUS) mutations disrupt Transportin-mediated nuclear import. EMBO J. 2010;29(16):2841–57.

50. Polymenidou M, Lagier-Tourenne C, Hutt KR, Huelga SC, Moran J, Liang TY, et al. Long pre-mRNA depletion and RNA missplicing contribute to neuronal vulnerability from loss of TDP-43 splicing of an intron within the 3' untranslated region of its own transcript, thereby triggering nonsense mediated RNA degradation. (147 words). Nat Neurosci. Nature Publishing Group; 2011;14(4):459–68.

51. Walker AK, Atkin JD. Stress signaling from the endoplasmic reticulum: A central player in the pathogenesis of amyotrophic lateral sclerosis. IUBMB Life. 2011;63(September):n/a – n/a.

52. Atkin JD, Farg M a., Walker AK, McLean C, Tomas D, Horne MK. Endoplasmic reticulum stress and induction of the unfolded protein response in human sporadic amyotrophic lateral sclerosis. Neurobiol Dis. Elsevier Inc.; 2008;30(3):400–7.

53. Atkin JD, Farg M a., Turner BJ, Tomas D, Lysaght J a., Nunan J, et al. Induction of the unfolded protein response in familial amyotrophic lateral sclerosis and association of protein-disulfide isomerase with superoxide dismutase 1. J Biol Chem. 2006;281(40):30152–65.

54. Zhao W, Beers DR, Appel SH. Immune-mediated mechanisms in the pathoprogression of amyotrophic lateral sclerosis. J Neuroimmune Pharmacol. 2013;8(4):888–99.

55. Fischer LR, Culver DG, Tennant P, Davis A a., Wang M, Castellano-Sanchez A, et al. Amyotrophic lateral sclerosis is a distal axonopathy: evidence in mice and man. Exp Neurol. 2004;185(2):232–40.

56. Cavanagh, J. B. The significance of the "dying back" process in human and experimental neurological diseases. Int Rev Exp. 1964;3:219–67.

57. Spencer, P S. Central-peripheral distal axonopathy - The pathogenisis of dying-back polyneuropathies. Prog Neuropathol. 1976;3:253–95.

58. Holzbaur ELF. Motor neurons rely on motor proteins. Trends Cell Biol. 2004;14(5):233–40.

59. Perlson E, Maday S, Fu M-M, Moughamian AJ, Holzbaur ELF. Retrograde axonal transport: pathways to cell death? Trends Neurosci. Elsevier Ltd; 2010;33(7):335–44.

60. Vos KJ De, Grierson AJ, Ackerley S, Miller CCJ. Role of Axonal Transport in Neurodegenerative Diseases. Annu Rev Neurosci. 2008;31:151–73.

61. Collard JF, Cote F, Julien JP. Defective axonal transport in a transgenic mouse model of amyotrophic lateral sclerosis. Nature. 1995. p. 61–4.

62. Perlson E, Jeong G-B, Ross JL, Dixit R, Wallace KE, Kalb RG, et al. A Switch in Retrograde Signaling from Survival to Stress in Rapid-Onset Neurodegeneration. J Neurosci. 2009;29(31):9903–17.

63. Ligon L a, LaMonte BH, Wallace KE, Weber N, Kalb RG, Holzbaur ELF. Mutant superoxide dismutase disrupts cytoplasmic dynein in motor neurons. Neuroreport. 2005;16(6):533–6.

64. Bommel H, Xie G, Rossoll W, Wiese S. Missense mutation in the tubulin-specific chaperone E (Tbce) gene in the mouse mutant progressive motor neuronopathy, a model of human motoneuron disease. J Cell Biol. 2002;159(4):563–9.

65. Sagot Y, Vejsada R, Kato AC, Sagot Y, Vejsada R, Kato AC. Clinical and molecular aspects of motoneurone diseases : animal models , neurotrophic factors and Bcl-2 oncoprotein. Trends Pharmacol. 1997;18:330–7.

66. Ferri A, Sanes, J R, Coleman, M P, Cunningham, J M, Kato, A C. Inhibiting axon degeneration and synapse loss attenuates apoptosis and disease progression in a mouse model of motorneuron disease. Curr Biol. 2003;13:669–73.

67. Ikenaka K, Katsuno M, Kawai K, Ishigaki S, Tanaka F, Sobue G. Disruption of axonal transport in motor neuron diseases. Int J Mol Sci. 2012;13(1):1225–38.

68. Hafezparast M, Klocke R, Ruhrberg C, Marquardt A, Ahmad-Annuar A, Bowen S, et al. Mutations in dynein link motor neuron degeneration to defects in retrograde transport. Science. 2003;300(5620):808–12.

69. LaMonte BH, Wallace KE, Holloway B a., Shelly SS, Ascaño J, Tokito M, et al. Disruption of dynein/dynactin inhibits axonal transport in motor neurons causing late-onset progressive degeneration. Neuron. 2002;34(5):715–27.

70. Humbert, Richard; David A. Adler, Christine M. Disteche, Christopher Hassett, Curtis J. Omiecinski CEF. Fusion of the dominant negative transcription regulator CHOP with a novel gene FUS by translocation (12;16) in malignant liposarcoma. Nat Genet. 1993;3:73–96.

71. Prasad DD, Ouchida M, Lee L, Rao VN, Reddy ES. TLS/FUS fusion domain of TLS/FUS-erg chimeric protein resulting from the t(16;21) chromosomal translocation in human myeloid leukemia functions as a transcriptional activation domain. Oncogene. 1994;9(12):3717–29.

72. Tan AY, Manley JL. The TET family of proteins: Functions and roles in disease. J Mol Cell Biol. 2009;1(2):82–92.

73. Peters OM, Ghasemi M, Brown RH. Emerging mechanisms of molecular pathology in ALS. J Clin Invest. 2015;125(5):1767–79.

74. Zinszner H, Sok J, Immanuel D, Yin Y, Ron D. TLS (FUS) binds RNA in vivo and engages in nucleo-cytoplasmic shuttling. J Cell Sci. 1997;110 (Pt 1:1741–50.

75. Sama RRK, Ward CL, Bosco D a. Functions of FUS/TLS From DNA Repair to Stress Response: Implications for ALS. ASN Neuro. 2014;6(4).

76. Kuroda M, Sok J, Webb L, Baechtold H, Urano F, Yin Y, et al. Male sterility and enhanced radiation sensitivity in TLS(-/-) mice. EMBO J. 2000;19(3):453–62.

77. Zhu H, Belcher M, van der Harst P. Healthy aging and disease: role for telomere biology? Clin Sci (Lond). 2011;120(10):427–40.

78. Meissner M, Lopato S, Gotzmann J, Sauermann G, Barta A. Proto-oncoprotein TLS/FUS is associated to the nuclear matrix and complexed with splicing factors PTB, SRm160, and SR proteins. Exp Cell Res. 2003;283(2):184–95.

79. Orozco D, Edbauer D. FUS-mediated alternative splicing in the nervous system: Consequences for ALS and FTLD. J Mol Med. 2013;91(12):1343–54.

80. Morlando M, Dini Modigliani S, Torrelli G, Rosa A, Di Carlo V, Caffarelli E, et al. FUS stimulates microRNA biogenesis by facilitating co-transcriptional Drosha recruitment. EMBO J. Nature Publishing Group; 2012;31(24):4502–10.

81. Fujii R, Okabe S, Urushido T, Inoue K, Yoshimura A, Tachibana T, et al. The RNA binding protein TLS is translocated to dendritic spines by mGluR5 activation and regulates spine morphology. Curr Biol. 2005;15(6):587–93.

82. Fiesel FC, Kahle PJ. TDP-43 and FUS/TLS: Cellular functions and implications for neurodegeneration. FEBS J. 2011;278(19):3550–68.

83. Dormann D, Haass C. Fused in sarcoma (FUS): An oncogene goes awry in neurodegeneration. Mol Cell Neurosci. Elsevier Inc.; 2013;56:475–86.

84. Hübers A, Just W, Rosenbohm A, Müller K, Marroquin N, Goebel I, et al. De novo FUS mutations are the most frequent genetic cause in early-onset German ALS patients. Neurobiol Aging. Elsevier Inc; 2015;36(11):3117.e1–3117.e6.

85. Mackenzie IR a, Rademakers R, Neumann M. TDP-43 and FUS in amyotrophic lateral sclerosis and frontotemporal dementia. Lancet Neurol. Elsevier Ltd; 2010;9(10):995–1007.

86. Zhang ZC, Chook YM. Structural and energetic basis of ALS-causing mutations in the atypical proline-tyrosine nuclear localization signal of the Fused in Sarcoma protein (FUS). Proc Natl Acad Sci. 2012;109(30):12017–21.

87. Kent L, Vizard TN, Smith BN, Topp SD, Vance C, Gkazi A, et al. Autosomal dominant inheritance of rapidly progressive amyotrophic lateral sclerosis due to a truncation mutation in the fused in sarcoma (FUS) gene. Amyotroph Lateral Scler Frontotemporal Degener. 2014;15(7-8):557–62.

88. Sama RRK, Ward CL, Kaushansky LJ, Lemay N, Ishigaki S, Urano F, et al. FUS/TLS assembles into stress granules and is a prosurvival factor during hyperosmolar stress. J Cell Physiol. 2013;228(11):2222–31.

89. Anderson P, Kedersha N. Stress granules: the Tao of RNA triage. Trends Biochem Sci. 2008;33(3):141–50.

90. Ramaswami M, Taylor JP, Parker R. Altered ribostasis: RNA-protein granules in degenerative disorders. Cell. Elsevier Inc.; 2013;154(4):727–36.

91. Patel A, Lee HO, Jawerth L, Maharana S, Jahnel M, Hein MY, et al. A Liquid-to-Solid Phase Transition of the ALS Protein FUS Accelerated by Disease Mutation. Cell. Elsevier Inc.; 2015;162(5):1066–77.

92. Schaefer A, O'Carroll D, Tan CL, Hillman D, Sugimori M, Llinas R, et al. Cerebellar neurodegeneration in the absence of microRNAs. J Exp Med. 2007;204(7):1553–8.

93. Tao J, Wu H, Lin Q, Wei W, Lu X-H, Cantle JP, et al. Deletion of Astroglial Dicer Causes Non-Cell-Autonomous Neuronal Dysfunction and Degeneration. J Neurosci. 2011;31(22):8306–19.

94. Nomura T, Watanabe S, Kaneko K, Yamanaka K, Nukina N, Furukawa Y. Intranuclear aggregation of mutant FUS/TLS as a molecular pathomechanism of amyotrophic lateral sclerosis. J Biol Chem. 2014;289(2):1192–202.

95. Yang L, Gal J, Chen J, Zhu H. Self-assembled FUS binds active chromatin and regulates gene transcription. PNAS. 2014;111(50):17809–14.

96. Julien J-P, Kriz J. Transgenic mouse models of amyotrophic lateral sclerosis. Biochim Biophys Acta. 2006;1762(11-12):1013–24.

97. Benatar M. Lost in translation: Treatment trials in the SOD1 mouse and in human ALS. Neurobiol Dis. 2007;26(1):1–13.

98. McGoldrick P, Joyce PI, Fisher EMC, Greensmith L. Rodent models of amyotrophic lateral sclerosis. Biochim Biophys Acta. Elsevier B.V.; 2013;1832(9):1421–36.

99. Dunckley T, Huentelman MJ, Craig DW, Pearson J V, Szelinger S, Joshipura K, et al. Whole-genome analysis of sporadic amyotrophic lateral sclerosis. N Engl J Med. 2007;357(8):775–88.

100. Takahashi K, Tanabe K, Ohnuki M, Narita M, Ichisaka T, Tomoda K, et al. Induction of Pluripotent Stem Cells from Adult Human Fibroblasts by Defined Factors. Cell. 2007;131(5):861–72.

101. Davis-Dusenbery BN, Williams L a, Klim JR, Eggan K. How to make spinal motor neurons. Development. 2014;141(3):491–501.

102. Dimos JT, Rodolfa KT, Niakan KK, Weisenthal LM, Mitsumoto H, Chung W, et al. Induced pluripotent stem cells generated from patients with ALS can be differentiated into motor neurons. Science (80-). 2008;321(5893):1218–21.

103. Sances S, Bruijn LI, Chandran S, Eggan K, Ho R, Klim JR, et al. Modeling ALS with motor neurons derived from human induced pluripotent stem cells. Nat Neurosci. 2016;19(4).

104. Hamburger V. The Heritage of Experimental Embryology: Hans Spemann and the Organizer. oxford Univ Press. 1988;

105. Stern CD. Neural induction: old problem, new findings, yet more questions. Development. 2005;132(9):2007–21.

106. Egawa N, Kitaoka S, Tsukita K, Naitoh M, Takahashi K, Yamamoto T, et al. Drug Screening for ALS Using Patient-Specific Induced Pluripotent Stem Cells. Sci Transl Med. 2012;4(145):145ra104–45ra104.

107. Bilican B, Serio A, Barmada SJ, Nishimura AL, Sullivan GJ, Carrasco M, et al. Mutant induced pluripotent stem cell lines recapitulate aspects of TDP-43 proteinopathies and reveal cell-specific vulnerability. Proc Natl Acad Sci U S A. 2012;109(15):5803–8.

108. Burkhardt MF, Martinez FJ, Wright S, Ramos C, Volfson D, Mason M, et al. A cellular model for sporadic ALS using patient-derived induced pluripotent stem cells. Mol Cell Neurosci. Elsevier Inc.; 2013;56:355–64.

109. Almeida S, Gascon E, Tran H, Chou HJ, Gendron TF, Degroot S, et al. Modeling key pathological features of frontotemporal dementia with C9ORF72 repeat expansion in iPSC-derived human neurons. Acta Neuropathol. 2013;126(3):385–99.

110. Donnelly CJ, Zhang PW, Pham JT, Heusler AR, Mistry N a., Vidensky S, et al. RNA Toxicity from the ALS/FTD C9ORF72 Expansion Is Mitigated by Antisense Intervention. Neuron. Elsevier; 2013;80(2):415–28.

111. Chen H, Qian K, Du Z, Cao J, Petersen A, Liu H, et al. Modeling ALS with iPSCs reveals that mutant SOD1 misregulates neurofilament balance in motor neurons. Cell Stem Cell. Elsevier Inc.; 2014;14(6):796–809.

112. Bruijn LI, Houseweart MK, Kato S, Anderson KL, Anderson SD, Ohama E, et al. Aggregation and motor neuron toxicity of an ALS-linked SOD1 mutant independent from wild-type SOD1. Science. 1998;281(5384):1851–4.

113. Wainger BJ, Kiskinis E, Mellin C, Wiskow O, Steve SW, Berry JD, et al. Intrinsic membrane hyperexcitability of ALS patient-derived motor neurons. Cell Rep. 2014;7(1):1–11.

114. Japtok J, Lojewksi X, Naumann M, Klingenstein M, Reinhardt P, Sterneckert J, et al. Stepwise acquirement of hallmark neuropathology in FUS-ALS iPSC models depends on mutation type and neuronal aging. Neurobiol Dis. Elsevier Inc.; 2015;82:420–9.

115. Lenzi J, De Santis R, de Turris V, Molando M, Laneve P, Calvo A, et al. ALS mutant FUS proteins are recruited into stress granules in induced pluripotent stem cell-derived motoneurons. Dis Model Mech. 2015;8(7):755–66.

116. Matus S, Medinas DB, Hetz C. Common ground: Stem cell approaches find shared pathways underlying ALS. Cell Stem Cell. Elsevier Inc.; 2014;14(6):697–9.

117. Maury Y, Côme J, Piskorowski R a, Salah-Mohellibi N, Chevaleyre V, Peschanski M, et al. Combinatorial analysis of developmental cues efficiently converts human pluripotent stem cells into multiple neuronal subtypes. Nat Biotechnol. 2014;33(1):89–96.

118. Sheng Z-H, Cai Q. Mitochondrial transport in neurons: impact on synaptic homeostasis and neurodegeneration. Nat Rev Neurosci. 2012;13(2):77–93.

119. Davis-Dusenbery BN, Williams L a, Klim JR, Eggan K. How to make spinal motor neurons. Development. 2014;141(3):491–501.

120. Amoroso MW, Croft GF, Williams DJ, O'Keeffe S, Carrasco M a, Davis a R, et al. Accelerated high-yield generation of limb-innervating motor neurons from human stem cells. J Neurosci. 2013;33(2):574–86.

121. Sareen D, O'Rourke JG, Meera P, Muhammad a KMG, Grant S, Simpkinson M, et al. Targeting RNA foci in iPSC-derived motor neurons from ALS patients with a C9ORF72 repeat expansion. Sci Transl Med. 2013;5(208):208ra149.

122. Devlin A-C, Burr K, Borooah S, Foster JD, Cleary EM, Geti I, et al. Human iPSC-derived motoneurons harbouring TARDBP or C9ORF72 ALS mutations are dysfunctional despite maintaining viability. Nat Commun. Nature Publishing Group; 2015;6:1–12.

123. Qu Q, Li D, Louis KR, Li X, Yang H, Sun Q, et al. High-efficiency motor neuron differentiation from human pluripotent stem cells and the function of Islet-1. Nat Commun. Nature Publishing Group; 2014;5:3449.

124. Fischer ES, Böhm K, Lydeard JR, Yang H, Stadler MB, Cavadini S, et al. HHS Public Access. Cell Stem Cell. 2015;512(7512):49–53.

125. Sun Y, Dykes IM, Liang X, Eng SR, Evans SM, Turner EE. A central role for Islet1 in sensory neuron development linking sensory and spinal gene regulatory programs. Nat Neurosci. 2008;11(11):1283–93.

126. Wilson JM, Hartley R, Maxwell DJ, Todd AJ, Lieberam I, Kaltschmidt JA, et al. Conditional Rhythmicity of Ventral Spinal Interneurons Defined by Expression of the Hb9 Homeodomain Protein. J Neurosci. 2005;25(24):5710–9.

127. Liu X, Chen J, Liu W, Li X, Chen Q, Liu T, et al. The fused in sarcoma protein forms cytoplasmic aggregates in motor neurons derived from integration-free induced pluripotent stem cells generated from a patient with familial amyotrophic lateral sclerosis carrying the FUS-P525L mutation. Neurogenetics. 2015;16(3):223–31.

128. Ichiyanagi N, Fujimori K, Yano M, Ishihara-Fujisaki C, Sone T, Akiyama T, et al. Establishment of In Vitro FUS-Associated Familial Amyotrophic Lateral Sclerosis Model Using Human Induced Pluripotent Stem Cells. Stem Cell Reports. The Authors; 2016;6(4):496–510.

129. Kaus A, Sareen D. ALS Patient Stem Cells for Unveiling Disease Signatures of Motoneuron Susceptibility: Perspectives on the Deadly Mitochondria, ER Stress and Calcium Triad. Front Cell Neurosci. 2015;9(November):448.

130. Philippidou P, Dasen JS. Hox Genes: Choreographers in Neural Development, Architects of Circuit Organization. Neuron. Elsevier Inc.; 2013;80(1):12–34.

131. Zou ZY, Cui LY, Sun Q, Li XG, Liu MS, Xu Y, et al. De novo FUS gene mutations are associated with juvenile-onset sporadic amyotrophic lateral sclerosis in China. Neurobiol Aging. Elsevier Ltd; 2013;34(4):1312.e1–1312.e8.

132. Huang EJ, Zhang J, Geser F, Trojanowski JQ, Strober JB, Dickson DW, et al. Extensive FUS-immunoreactive pathology in juvenile amyotrophic lateral sclerosis with basophilic inclusions. brain pathol. 2010;20(6):1069–76.

133. Leblond CS, Webber a., Gan-Or Z, Moore F, Dagher a., Dion P a., et al. De novo FUS P525L mutation in Juvenile amyotrophic lateral sclerosis with dysphonia and diplopia. Neurol Genet. 2016;2(2):e63–e63.

134. Shang Y, Huang EJ. Mechanisms of FUS mutations in familial amyotrophic lateral sclerosis. Brain Res. Elsevier; 2016;1–14.

135. Vance C, Scotter EL, Nishimura AL, Troakes C, Mitchell JC, Kathe C, et al. ALS mutant FUS disrupts nuclear localization and sequesters wild-type FUS within cytoplasmic stress granules. Hum Mol Genet. 2013;22(13):2676–88.

136. Murakami T, Yang SP, Xie L, Kawano T, Fu D, Mukai A, et al. Als mutations in FUS cause neuronal dysfunction and death in caenorhabditis elegans by a dominant gain-of-function mechanism. Hum Mol Genet. 2012;21(1):1–9.

137. Duffy LM, Chapman a. L, Shaw PJ, Grierson a. J. The role of mitochondria in the pathogenesis of amyotrophic lateral sclerosis. Neuropathol Appl Neurobiol. 2011;37(4):336–52.

138. Baldwin KR, Godena VK, Hewitt VL, Whitworth AJ. Axonal transport defects are a common phenotype in Drosophila models of ALS. oxford Univ Press. 2016;

139. Lee S, Sato Y, Nixon R a. Lysosomal proteolysis inhibition selectively disrupts axonal transport of degradative organelles and causes an Alzheimer's-like axonal dystrophy. J Neurosci. 2011;31(21):7817–30.

140. Maday S, Twelvetrees AE, Moughamian AJ, Holzbaur ELF. Axonal Transport: Cargo-Specific Mechanisms of Motility and Regulation. Neuron. Elsevier Inc.; 2014;84(2):292–309.

141. Maday S, Wallace KE, Holzbaur ELF. Autophagosomes initiate distally and mature during transport toward the cell soma in primary neurons. J Cell Biol. 2012;196(4):407–17.

142. Yang Y, Coleman M, Zhang L, Zheng X, Yue Z. Autophagy in axonal and dendritic degeneration. Trends Neurosci. Elsevier Ltd; 2013;36(7):418–28.

143. Wong YC, Holzbaur ELF. Autophagosome dynamics in neurodegeneration at a glance. J Cell Sci. 2015;128(7):1259–67.

144. Harris H, Rubinsztein DC. Control of autophagy as a therapy for neurodegenerative disease. Nat Rev Neurol. Nature Publishing Group; 2011;8(2):108–17.

145. Xie Y, Zhou B, Lin MY, Wang S, Foust KD, Sheng ZH. Endolysosomal Deficits Augment Mitochondria Pathology in Spinal Motor Neurons of Asymptomatic fALS Mice. Neuron. Elsevier Inc.; 2015;87(2):355–71.

146. Groen EJN, Fumoto K, Blokhuis AM, Engelen-Lee JY, Zhou Y, van den Heuvel DM a, et al. ALS-associated mutations in FUS disrupt the axonal distribution and function of SMN. Hum Mol Genet. 2013;22(18):3690–704.

147. Gerbino V, Carrì MT, Cozzolino M, Achsel T. Mislocalised FUS mutants stall spliceosomal snRNPs in the cytoplasm. Neurobiol Dis. Elsevier Inc.; 2013;55:120–8.

148. Garcera a, Bahi N, Periyakaruppiah a, Arumugam S, Soler RM. Survival motor neuron protein reduction deregulates autophagy in spinal cord motoneurons in vitro. Cell Death Dis. Nature Publishing Group; 2013;4(6):e686.

149. Xu C, Denton KR, Wang Z, Zhang X, Li X. Abnormal mitochondrial transport and morphology as early pathological changes in human models of spinal muscular atrophy. Dis Model Mech. 2016;9:39–49.

150. Pierzynska-Mach A, Janowski P a., Dobrucki JW. Evaluation of acridine orange, LysoTracker Red, and quinacrine as fluorescent probes for long-term tracking of acidic vesicles. Cytom Part A. 2014;85(8):729–37.

151. Cai Q, Lu L, Tian J, Zhu Y, Qiao H, Sheng Z. Snapin-Regulated Late Endosomal Transport Is Critical for Efficient Autophagy-Lysosomal Function in Neurons. Neuron. 2010;68:73–86.

152. Chen H, Qian K, Du Z, Cao J, Petersen A, Liu H, et al. Modeling ALS with iPSCs Reveals that Mutant SOD1 Misregulates Neurofilament Balance in Motor Neurons. Cell Stem Cell. Elsevier Inc.; 2014;14(6):796–809.

153. Magrané J, Cortez C, Gan W-B, Manfredi G. Abnormal mitochondrial transport and morphology are common pathological denominators in SOD1 and TDP43 ALS mouse models. Hum Mol Genet. 2014;23(6):1413–24.

154. Daigle GG, Lanson N a., Smith RB, Casci I, Maltare A, Monaghan J, et al. Rna-binding ability of FUS regulates neurodegeneration, cytoplasmic mislocalization and incorporation into stress granules associated with FUS carrying ALS-linked mutations. Hum Mol Genet. 2013;22(6):1193–205.

155. Miller J, Ganat YM, Kishinevsky S, Bowman RL, Liu B, Tu EY, et al. Human iPSC-based modeling of late onset disease via progerin-induced aging. 2013. 691-705 p.

156. Colombrita C, Onesto E, Megiorni F, Pizzuti A, Baralle FE, Buratti E, et al. TDP-43 and FUS RNA-binding proteins bind distinct sets of cytoplasmic messenger RNAs and differently regulate their post-transcriptional fate in motoneuron-like cells. J Biol Chem. 2012;287(19):15635–47.

157. Hoell JI, Larsson E, Runge S, Nusbaum JD, Duggimpudi S, Farazi T a, et al. RNA targets of wild-type and mutant FET family proteins. Nat Struct Mol Biol. Nature Publishing Group; 2011;18(12):1428–31.

158. Edgar JM, Nave KA. The role of CNS glia in preserving axon function. Curr Opin Neurobiol. 2009;19(5):498–504.

159. Haidet-Phillips AM, Gross SK, Williams T, Tuteja A, Sherman A, Ko M, et al. Altered astrocytic expression of TDP-43 does not influence motor neuron survival. Exp Neurol. Elsevier Inc.; 2013;250:250–9.

160. Serio A, Bilican B, Barmada SJ, Ando DM, Zhao C, Siller R, et al. Astrocyte pathology and the absence of non-cell autonomy in an induced pluripotent stem cell model of TDP-43 proteinopathy. Proc Natl Acad Sci U S A. 2013;110(12):4697–702.

161. Jacquier a., Bellouze S, Blanchard S, Bohl D, Haase G. Astrocytic protection of spinal motor neurons but not cortical neurons against loss of Als2/alsin function. Hum Mol Genet. 2009;18(12):2127–39.

162. Chandran J, Ding J, Cai H. Alsin and the molecular pathways of amyotrophic lateral sclerosis. Mol Neurobiol. 2007;36(3):224–31.

Supplementary data

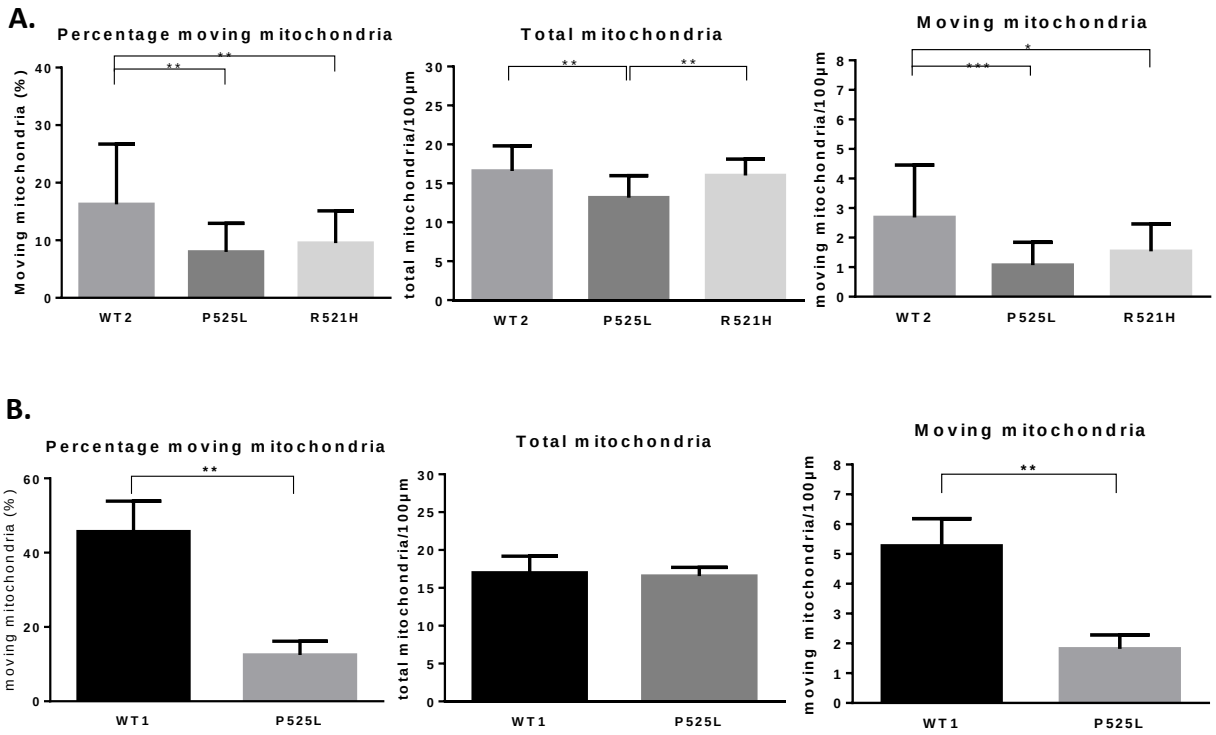

Supplementary figure 1. Mitochondrial transport data. Quantification of **(left)** the percentage of moving mitochondria, **(middle)** total mitochondria per 100µm and **(right)** moving mitochondria per 100µm. Mitochondrial transport was analyzed at day 32 of the differentiation protocol with the use of a MyoTracker staining. Two independent differentiations are shown. **(A)** Data performed by myself. **(B).** Data performed by PhD-student of the neurobiology lab Wenting Guo. Data are represented as mean ± SD. * = $P < 0.05$; ** = $P < 0.01$; *** = $P < 0.005$. Number of measured neurites: **(A)** WT1 = 15; WT2 = 4; FUS P525L= 22; FUS R521H= 25. **(B)** WT1= 6; FUS P525L = 6